

1 Dear Dr. Evans,

2

3 Thank you for the constructive comments we received on our manuscript. Below, all comments
4 are listed in italics. We try to answer all specific comments raised by your review (in bold).

5

6 *Trans-membrane-transport is not required to explain these results, therefore a discussion of*
7 *how they would be interpreted in terms of seawater vacuolisation should be included.*

8 **We agree with the reviewer that our results are not providing conclusive evidence for**
9 **either one of the current biomineralization concepts, seawater endocytosis and TMT**
10 **mixing. Still, the different observed correlations between the incorporation of trace**
11 **elements in hyaline and porcelaneous species are best explained by primarily**
12 **vacuolization in porcelaneous and a mixed signal in hyaline species. To accommodate the**
13 **reviewers concern we now included a paragraph in which we evaluate the effect of the**
14 **potential contribution of vacuolized seawater using our observations. The discussion now**
15 **includes a comparison of the relative low (hyaline) and high (porcelaneous) contribution**
16 **of vacuolized seawater on overall EI/Ca.**

17

18 • *Although to my knowledge it remains to be tested, it is likely that the extent to which*
19 *foraminifera raise the pH of seawater vacuoles is dependent on the ambient seawater pH (also*
20 *by analogy to the ECF in corals). Therefore, seawater pH can be expected to influence (e.g.)*
21 *Zn and Ba speciation in the seawater vacuole. Because a certain species is probably*
22 *preferentially incorporated during crystal growth, there is no need to invoke poorly selective*
23 *channels or pumps (lines 311-315).*

24 **How (if at all) the internal pH of foraminifera depends on seawater pH outside the**
25 **foraminifer, is currently not known. If it does change in concert, the internal pH at the**
26 **site of calcification (which is ≥ 9 ; De Nooijer et al, 2009) would vary between >9 and >8.6**
27 **in our study. In theory such a change in internal pH from >9 to >8.6 changes $[\text{CO}_3^{2-}]$ and**
28 **thus the speciation of e.g. Zn and Ba at the site of calcification. However, over this range**
29 **the change in $[\text{CO}_3^{2-}]$ will be rather limited. Hence such an effect of differential speciation**
30 **within the calcifying fluid does not suffice to explain the observed sensitivity in Zn and Ba**
31 **to pCO_2 in our study. This is in line with recent evidence on Zn/Ca in foraminifera, which**
32 **suggests Zn incorporation is not governed by changes in seawater pH, but by carbonate**
33 **ion concentration which does not change very much anymore at these high pH's (van Dijk**
34 **et al., 2017, figure 5d).**

35

36 • *Given that the Mg distribution coefficient for some species is greater than that of inorganic*
37 *calcite, it is difficult to see how TMT helps explain the geochemistry of these foraminifera. In*
38 *fact, it causes problems. If these species are still sourcing a portion of the Ca through channels*
39 *or pumps (lines 309- 311 and 362-364), then presumably the Mg/Ca ratio of the calcifying fluid*

40 *is lower than that of seawater, yet in some cases they precipitate calcite with a Mg/Ca ratio ~3*
41 *times that of inorganic calcite. There are three species shown in Figure 3 with a Mg/Ca ratio*
42 *twice that of the highest Mg/Ca species of this study. A different mechanism is required here,*
43 *and it is unclear how TMT could fit into this given it would require pumping Ca out of seawater*
44 *to raise the Mg/Ca ratio before precipitation. In contrast to what is stated on C2 lines 357-359,*
45 *the highest Mg species are equally (or even more) different from inorganic calcite as the low-*
46 *Mg species.*

47 **If the D of the foraminifera would be higher, this would indeed be true. However, we**
48 **apologize for erroneously plotting the wrong inorganic D for Mg, which should have been**
49 **~150-200 (Mucci and Morse, 1983; Morse et al., 2007), indicating that all known**
50 **foraminiferal partition coefficients are well below the inorganic D. We refrain from**
51 **replotting this based on the next comment of this reviewer. Still, to accommodate this**
52 **reviewers' concerns we extended our discussion, as mentioned above, to now also include**
53 **other mechanisms potentially contributing to transport of ions to the SOC.**

54

55 2. Figure 3. The inorganic calcite distribution coefficients should only be displayed if they were
56 characterised from calcite precipitated from seawater. For example, the sodium distribution
57 coefficient is based on solutions with a chemistry very different from that of seawater, most
58 notably the Mg concentration was much lower. It is coincidence that it is roughly the same as
59 the miliolids and does not suggest that they precipitate shells with a similar D_{Na} to that of
60 inorganic calcite in seawater (lines 360-361). It is well known that Mg exerts a control on trace
61 element distribution coefficients (see below), therefore it is not representative to compare these
62 results to inorganic precipitation where these are carbonates precipitated from non-seawater
63 solutions.

64 **We have removed the inorganic D's from figure 3, since the inorganically precipitated**
65 **calcites are usually not derived from (natural) seawater. Most inorganic precipitation**
66 **experiments do not utilize seawater as a source for carbonate precipitation, as it**
67 **complicates the design of the experiment. This makes a direct comparison with**
68 **foraminiferal calcite impossible.**

69

70 3. Section 4.1 and Figure 3. The reason that trace element distribution coefficients are strongly
71 positively correlated with D_{Mg} is because the incorporation of Mg into calcite modifies the
72 incorporation of other elements through the associated lattice distortion. For example, this has
73 been shown in inorganic calcite in the case of D_{Sr} [Mucci & Morse, 1983] and D_{Na} [Okumura
74 & Kitano, 1986], and we confirmed that this is also the case in foraminifera through cultures in
75 variable seawater Mg/Ca [Evans et al., 2015]. The point is that this effect is not a consequence
76 of ion transport, but has a basis in crystallography, especially given that hyaline foraminifera
77 lie on the same DX-Mg/Ca calcite line as inorganic precipitates [see Evans et al., 2015 Fig. 7].
78 Furthermore, the trace element distribution coefficients shown in Figure 3 would be better
79 expressed as a function of the calcite Mg/Ca ratio rather than D_{Mg}. It will not make much
80 difference as most of these data are from foraminifera grown in seawater with a Mg/Ca ratio

81 close to that of modern, but mechanistically it is the Mg concentration of calcite that is
82 important.

83 **We agree that Mg incorporation might distort the calcite crystal lattice, allowing for a**
84 **higher incorporation of for instance Sr and Na. Some of us were actually actively involved**
85 **in studies specifically targeting this (e.g. Mewes et al., 2015). In the new version of our**
86 **manuscript we now emphasized this issue by add a paragraph (in 4.2), mentioning that**
87 **this interdependency of element incorporation on Mg has been observed in both inorganic**
88 **and culture experiments, and might partly stem from crystallography. However, although**
89 **this mechanism might explain some of the observed species specific element incorporation**
90 **in hyaline foraminifera, this does not explain the difference between hyaline and**
91 **porcelaneous foraminifera. Porcelaneous foraminifera have in general high Mg/Ca, but**
92 **we actually observe lower incorporation of Na and Sr compared to hyaline species with**
93 **similar DMg (Fig 3, upper right and left panel: DMg versus DNa and DSr). When**
94 **including porcelaneous species from other studies we also observe no increase in DSr over**
95 **a larger range in DMg (Fig 3, upper left panel: DMg versus DSr). This indicates that the**
96 **mechanisms (or mechanisms) might be very different for hyaline and porcelaneous**
97 **species, which is discussed in more detail at the end of our revised discussion.**

98 **We plotted partitioning coefficients rather than element to calcium ratios since a couple**
99 **of the published studies changed the Mg/Ca of the culture media, and this makes it easier**
100 **for readers to evaluate their own or other data.**

101

102 3. Lines 268-270. It is true that some benthic species show little response of Mg/Ca and Sr/Ca
103 to the carbonate system, but the $[\text{CO}_2-3]$ effect on some deep benthic foraminifera Mg/Ca is
104 well known. These are also low-Mg so this statement is not accurate.

105 **For deep sea species benthic foraminifera, observed response to changes in carbonation**
106 **ion concentration are mainly due to calcification in undersaturated seawater, as described**
107 **by ‘the carbonate ion saturation hypothesis’ (Elderfield et al., 2006) and also observed for**
108 **Zn by Marchitto et al., (2000, 2005) and Cd and Ba by McCorkle et al. (1995). We now**
109 **added this references and a few sentences on the carbonate ion effect in undersaturated**
110 **water to the revised discussion (4.1). However, there is some evidence that Sr**
111 **incorporation is directly influenced by the carbonate system (also shown by Keul et al., in**
112 **press). Still, sensitivity of Sr/Ca to e.g. $[\text{CO}_3^{2-}]$ is rather low (Keul et al., in press; van Dijk**
113 **et al., 2017). In our experiment the change in $[\text{CO}_3^{2-}]$ between the highest and lowest pCO_2**
114 **treatment is rather limited (90-220 $\mu\text{mol/kg}$), resulting in no observed correlation of Sr/Ca**
115 **with pCO_2**

116 4. Lines 277-279. There is no significant correlation between Mg/Ca and either DIC or
117 alkalinity in these studies.

118 **We removed this statement from the discussion section and state there is a correlation**
119 **between Mg/Ca and the carbonate system for planktonic foraminifera.**

120 5. Lines 283-285. It is not really the case that there is a trend between Ba/Ca and the carbonate
121 system in the planktonic cultures of Honisch et al. [2011]. Only the lowest pH cultures suggest
122 any trend, but there are no replicates of these. How does the difference between these results
123 and those presented here fit into the authors preferred biomineralisation model?

124 **If incorporation of Ba depends on speciation due to differences in $[\text{CO}_3^{2-}]$, we expect**
125 **plateauing of free Ba^{2+} when we model speciation for lower pCO_2 conditions (higher**
126 **$[\text{CO}_3^{2-}]$). This is in line with the reviewers comments.**

127 7. Lines 334-335. I don't understand this statement. Do you mean that the selectivity of these
128 channels depends on the amount of ions transported? Is there any evidence for this? It is more
129 intuitive that selectivity is not changing.

130 **We have re-written this section of our discussion. We agree with the referee that the**
131 **second explanation is more logical/intuitive, with the amount of Ca^{2+} in the vicinity of the**
132 **foraminifer decreasing, the relative element to calcium ratio of the seawater around the**
133 **foraminifera increases. This would result in a higher transport of elements other than**
134 **Ca^{2+} .**

135 8. Figure 3. There is a plotting mistake in the DNa panel. *P. acervali* and *H. antillarum* are
136 shown with different sodium distribution coefficients but the data in Table 3 indicate that they
137 are the same in both species.

138 **This is actually a mistake in the table. *P. acervali* has a DMg of 0.46 (also reflected in the**
139 **higher Mg/Ca_{CALCITE})**

140 9. Figure 5. I understand the logic for plotting this as a function of pCO_2 , but given that pH is
141 what we are able to reconstruct with boron isotopes I suggest adding a second set of x-axes to
142 enable the two to be easily related. It would also be interesting to extend this plot to include the
143 pH at the calcification site.

144 **We added a second x-axis to this figure, with the corresponding pH from our culture**
145 **study. We are not able to plot pH at the calcification site, since it is unknown how internal**
146 **pH responses to changes in ambient pH.**

147 10. Figure 6. Half of this figure could be cut as both panels essentially show the same thing. Or,
148 panel B could be replaced with a schematic showing how these results would fit into a
149 biomineralisation model wherein the ions are sourced through seawater vacuolisation.

150 **We adapted this figure to our revised discussion, and use it to show the contribution of**
151 **both mechanisms to fit our observations.**

152

153 Dear Dr Fujita,

154

155 Thanks for the thorough reading of our manuscript and your constructive comments

156 In general, the main concern of this referee was the focus of the manuscript, which should be
157 more towards the potential of Zn/Ca and Ba/Ca as carbonate system proxies. By changing and
158 restructuring the introduction and discussion session, we shifted the focus of the manuscript
159 more towards the changes in Zn and Ba incorporation as a function of $p\text{CO}_2$. The conclusions
160 and abstract are changed accordingly. Another one of the suggestions by both reviewers is to
161 broaden the discussion by including other biomineralization and ion transport models to explain
162 the species-specific trends in element incorporation.

163 The comments of the referee are posted below in italics. We address these issues point by point,
164 in bold.

165

166 *General comments:*

167 *1) Authors should reconsider what is the main purpose (hypothesis), what is the main results,*
168 *and what are conclusions obtained from this study. In the Introduction, you may need more*
169 *elegant story to explain why you conducted $p\text{CO}_2$ controlled experiments as well as why you*
170 *used symbiotic tropical large benthic foraminifera for this study, to understand trace element*
171 *incorporation in foraminifera. I think the main important results in this study were increasing*
172 *some trace element incorporation (Zn, Ba) with high $p\text{CO}_2$ environments and a chemical model*
173 *to explain this phenomenon.*

174 **Based on this comment we now somewhat changed the focus of the introduction more**
175 **towards carbonate system proxies (e.g. Zn/Ca) and the necessity to study this across**
176 **different taxa since they are known to 1) have different calcification mechanism and 2) a**
177 **different D for elements studied so far. We used tropical foraminifera since they have a**
178 **higher variability in Mg incorporation and both porcelaneous and hyaline species are**
179 **readily available in this region.**

180 **This also led to a reorganization of the discussion. First, we now discuss the Zn- and Ba-**
181 **incorporation as a function of $p\text{CO}_2$ (now 4.2) and then discuss overall differences between**
182 **hyaline and porcelaneous foraminifera (4.1 in the old manuscript). Then, we discuss the**
183 **chemical speciation of ions as a function of $p\text{CO}_2$ (4.3). Finally, we evaluate existing**
184 **biomineralization models based on our results.**

185 *2) Authors are mainly concerned about a correlation, but not dealt with the quantity (amount)*
186 *of elemental incorporation in foraminiferal calcite. Even if both Zn and Ba ion availability*
187 *increases with high $p\text{CO}_2$ conditions, the amount incorporated in foraminiferal calcite differs*
188 *between the two elements (Zn is four times more incorporated than Ba). We know that ionic*
189 *radius is related to trace element incorporation in calcite from many inorganic studies. How*
190 *does your chemical model explain the incorporation of elements quantitatively?*

191 **We now added these observations to the discussion. Following the TMT mixing model,**
192 **selectivity of Ca²⁺ channel differs for different elements, which probably also reflects in**
193 **part ionic radius (see also, Nehrke et al., 2013).**

194 *3) This paper is not discussed anywhere (only briefly mentioned in the Introduction) about*
195 *effects of temperature on element incorporation in foraminifera, which are well established by*
196 *many papers. In Figure 3, you compared results of your study with those of previous similar*
197 *studies. However, I wonder these results are not simply comparable because of different species*
198 *from different environments (water depths and latitudes, i.e. different temperature and salinity*
199 *ranges) as shown in Supplementary Table S1. Temperature effects should be normalized to*
200 *compare real DMg between different foraminiferal species. In addition, authors should discuss*
201 *the relative sensitivity on E/Ca between temperature and carbonate chemistry when both*
202 *parameters are variable.*

203 **We changed figure 3, to show the data of our study only. The previous figure 3 is now**
204 **moved to the supplementary info, and we excluded data from foraminifera**
205 **cultured/grown at low temperature, as they might partly have been grown under**
206 **undersaturated conditions with respect to calcite. Resulting species are all grown/cultured**
207 **in a temperature range of 18-29 °C. We did not correct E/Ca for temperature, since the**
208 **this effect on Na/Ca, Ba/Ca and Sr/Ca is not well constrained or unknown.**

209 *4) This study assumes only Ca-channel model as a possible ion transport mechanism. However,*
210 *other possible mechanisms of ion transport have been proposed in foraminifera. I suggest that*
211 *authors compare advantages and disadvantages of several transport models and justify the Ca*
212 *channel model as the most appropriate to explain results in this study.*

213 **This issue was also raised by the second reviewer. The discussion is now put in a somewhat**
214 **broader context, in which we also include other transport models, including seawater**
215 **vacuolization (e.g. Ter Kuile and Erez, 1991; Erez, 2003, Elderfield et al., 1996; De Nooijer**
216 **et al., 2014). This is added as a separated paragraphs in which we try to test/validate these**
217 **models with our observations.**

218 *5) I wonder if laser abrasion (LA) method is appropriate for biocalcification study. As you*
219 *know, hyaline foraminiferal shells are composed of the primary layer and the secondary layers*
220 *(coating) with the organic matrix. The LA method cannot discriminate differences in element*
221 *incorporation between these different layers. In addition, the spatial heterogeneity of E/Ca*
222 *among calcite crystals in a chamber wall has been reported by many studies. How do authors*
223 *overcome these problems by using the LA method?*

224 **Heterogeneity of elements in the chamber wall has only been observed in hyaline species,**
225 **since they have (bi)laminar calcification. In this study we incubated adult foraminifera in**
226 **culture media with calcein. LA-ICP-MS allows for targeting new chambers only, of which**
227 **all layers of calcite were formed during the experiment. By using LA-ICP-MS we obtain**
228 **an average signal of the chamber wall, averaging out any potential banding. Analysis of**
229 **sufficient specimens/ chambers reduces uncertainty in average e.g. Mg/Ca values.**
230 **Furthermore, we only ablated the final ~3 chambers, minimizing the potential effects of**

231 **varying number of test carbonate layers. First paragraph of the discussion now lists this**
232 **as one of the potential causes for element to calcium ratio (E/Ca) variability.**

233 *6) What kinds of other trace elements except for those examined in this study are sensitive to*
234 *pCO₂ based on the chemical model? That is useful information to find new proxies for paleo-*
235 *pCO₂. In addition, I wonder what cause differences between sensitive and insensitive elements*
236 *on pCO₂.*

237 **In this model we only looked at elements which we also measured by LA-ICP-MS. We**
238 **modelled the elements which based on their known geochemical behaviour are the most**
239 **likely to show differences as a function of changes in carbonate chemistry. All elements**
240 **have been modelled in some sort of other study previously as well (e.g. Keul et al., 2013).**
241 **When considering the impact of [CO₃²⁻] chemical speciation, the observed lack of**
242 **sensitivity for Sr, Na and Mg might stem from their high concentration in seawater**
243 **compared to e.g. Zn. Only a small amount of ions are hence complexed by [CO₃²⁻]. Since**
244 **there is a higher total amount of e.g. Mg ions in seawater, the amount of Mg-CO₃**
245 **complexation is relatively low. Due to their low concentrations and great affinity for**
246 **carbonate ions, elements like Cu, Co, Ni, Li, may be affected in the same way. We have**
247 **added the possible behavior of these elements according to changes in speciation (4.3,**
248 **chemical speciation).**

249

250 *7) Authors are confused about the terminology of Foraminifera. Throughout the text, the*
251 *authors used “hyaline” and “miliolid” as comparable terms. But the term “hyaline” indicates*
252 *the quality of shell appearance and the term “miliolid” is a taxon name belonging to the Order*
253 *Miliolida. I suggest authors use comparable terms of “hyaline vs. porcelaneous” as shell*
254 *appearance, “perforate vs. imperforate” as shell perforation, and “rotaliid vs. miliolid” as the*
255 *two main taxonomic groups.*

256 **To avoid any confusion, we changed the terminology in our paper to hyaline vs.**
257 **porcelaneous and perforate vs. imperforate.**

258

259 L1: Title is vague and general, should be changed to include keywords and reflect the main
260 results of this paper; for example, Calcification model of some trace element (Zn, Ba)
261 incorporation in foraminifera under high pCO₂ environments.

262 **We changed the title to: ‘Trends in element incorporation in hyaline and porcelaneous**
263 **foraminifera as a function of pCO₂’ to better cover our main results.**

264

265 *Introduction:*

266 *L38-40: This sentence is strictly speaking incorrect. Diverse miliolid foraminifera belonging to*
267 *larger benthic foraminifera (LBF) are found particularly in the Atlantic and the Caribbean. In*

268 addition, LBF do not cover a large Mg/Ca range, but only intermediate and high Mg/Ca ranges.
269 The authors have to explain advantages to use LBFs for their study in more detail.

270 **In our study we use intermediate to high Mg/Ca_{CALCITE} (in our study ranging from 28.5**
271 **(*A. carinata*) to 141.3 (*H. antillarum*) mmol/mol), which is a large range in Mg/Ca_{CALCITE}.**

272 **New text: “A number of larger benthic foraminifera form hyaline shells, although the**
273 **amount of Mg in their shells is often more than 10 times higher than that of planktonic**
274 **and small benthic hyaline species, hence covering a larger range in Mg/Ca_{CALCITE} values.”**

275

276 *Methods:*

277 L86: 90-600 μm fraction is too small for larger benthic foraminifers (almost juveniles).

278 **We picked both directly from the macroalgae and from the 90-600 μm fraction, we now**
279 **explain this in the methodology.**

280 L86: As far as I know, *Marginopora vertebralis* (Quoy & Gaimard) is not distributed in the
281 Caribbean and Atlantic (see Langer and Hottinger, 2000 *Micropaleontology*). Recheck if
282 identification is correct.

283 **We rechecked the identification of all of our species, and found that we misidentified**
284 ***Sorites marginalis* as *Marginopora vertebralis*. This is now changed in the revised version**
285 **of our manuscript.**

286 L55: Is a paper in review OK to cite? If it is OK, it should be listed in the Reference.

287 L60: Not listed in the Reference.

288 L150, (Nardeli et al., 2016): not listed in the Reference.

289 L154, Barker et al. (2003): not listed in the Reference.

290 L94: Where is “Chapter 7 ”? I also found other chapters in the text somewhere.

291 **5 points above: We removed all references to chapters and manuscripts in review**

292 L97-98: Add $p\text{CO}_2$ unit. Explain what (A) means.

293 **We added the $p\text{CO}_2$ unit (ppm) and explain the treatment names A-D**

294 L108-109: Add the precision of temperature control.

295 **The average temperature over the whole experiment was $25\pm 0.2^\circ\text{C}$, which is now added**
296 **to the revised manuscript.**

297 L110-111: Note the light intensity level. In addition, I wonder if LEDs and yellow culture bottles
298 (Fig. 1) affect wave length and hence the growth of symbiotic foraminifers?

299 **The culture bottles themselves are not yellow, it’s the calcein added to the culture media.**
300 **Almost all incubated foraminifera grew new chambers.**

301 *L113: Does food affect water quality and chemical composition?*

302 **The described *dunaliella* feeding solutions do not change the chemical composition, since**
303 **these *dunaliella* were rinsed, centrifuged, freeze-dried and subsequently diluted in the**
304 **culture media. Water was replaced every four days to keep organic waste buildup at a**
305 **minimum**

306 *L155: Could the organic matrix in a shell be removed by this method? Does data not include*
307 *any elemental incorporation in the organic matrix?*

308 **In this cleaning step we remove the organic matrix from the foraminiferal shells.**
309 **Although, in theory, it might be possible there are small amounts of matrix remaining in**
310 **the carbonates, the amount of organic matter in foraminiferal shells is low, even before**
311 **cleaning (e.g. 0.1-0.2 wt% of the total shell of *Heterostigina depressa*; wenier and Erez,**
312 **1984). However, for future work it might be interesting to analyze the organic matrix, to**
313 **evaluate its potential contribution to the total E/Ca.**

314 *L167: What is the main difference between this paper and Van Dijk et al. (in review)?*

315 **We removed this reference, since this article is still in review. The differences with this**
316 **study and Reichart et al. (2003) are summarized in this paragraph. For instance, we use**
317 **different ICP-MS's, different cells, and used additional standards.**

318

319 Results:

320 *L217-218: Explain the rationale (hypothesis) why the authors compare Mg/Ca with other*
321 *TE/Ca?*

322 **We included this figure in our manuscript because of the observed link between Mg and**
323 **other TE published earlier (like e.g. Evans et al., 2015).**

324 *L218-219: not only significant values, but also R² values should be noted.*

325 **The R² values are presented in Table 3**

326

327 Discussion:

328 *L249-251: Compare advantages and disadvantages of several ion transport models and justify*
329 *a Ca-channel model as the most appropriate to explain results in this study.*

330 *L260: I think miliolid foraminifera still need the major removal of Mg ions even if carbonate is*
331 *directly precipitated from seawater.*

332 **We broaden the discussion to include also other transport models and how these might**
333 **differ for porcelaneous and hyaline species, when comparing them to our observations.**

334 *L289: PHREEQC needs explanation*

335 *L290: Ilnl database?*

336 **PHREEQC and the llnl database are now explained in more detail in the new paragraph**
337 **4.3, which focusses on the modelling of chemical speciation.**

338 *Section 4.3: this section is mostly a review of previous studies. I suggest that authors explain*
339 *an incorporation model shown in Fig. 6 in detail.*

340 **Due to a reorganization in our discussion, we now spent two paragraphs on different**
341 **transport models.**

342 *Section 4.4: Does size matter? authors mentioned that they measured only small size (L86).*
343 *Calcarinids (Neorotalia in #15 in Fig. 3) are similar in size to Amphistegina, but have high Mg*
344 *contents similar to a bigger Heterostegina. You may need another interpretation to explain the*
345 *difference between two taxa. In addition, I think larger benthic foraminifers (in particular some*
346 *taxa dwelling at a lower euphotic depth) have a strategy to attain a high surface area to volume*
347 *ratio by flattening to get light for algal C6 symbionts. Please show the surface area to volume*
348 *ratio between comparing taxa to justify your interpretations. Less Ca channels in the membrane*
349 *of LBFs are also unlikely, because LBFs are bigger thus have much more membranes and*
350 *channels than smaller foraminifers if channel density are the same. I think the second process*
351 *is more feasible than the first process.*

352 *L347-350: I think this explanation is more plausible. Hyaline foraminifers are highly diverse*
353 *and may have similar but slightly different calcification strategy acquired during evolution. I*
354 *guess the relative contributions of primary and secondary layers and organic matrix may*
355 *depend on hyaline foraminiferal taxa, which may cause interspecific variability of E/Ca*
356 *compositions.*

357 **We removed this part of our discussion, since we agree it is the less likely explanation of**
358 **our observations for hyaline species. We end our discussion with a paragraph on the**
359 **contribution of different mechanisms, which might explain our observations for both**
360 **hyaline and porcelaneous species.**

361 *Section 4.5. L359: I think the major removal of Mg is necessary because your results show that*
362 *DMg is much lower than 1.*

363 **With the seawater vacuolization model (Erez, 2003) it is indeed necessary to remove Mg**
364 **ions from the calcification fluid. But the removal of Mg is not necessary when ions are**
365 **transported by TMT, since these channels mainly import Ca to the site of calcification.**
366 **Only very few Mg ions would be transported (1 for every 10.000 Ca ions).**

367 *L366-369: Is this correct? lower? I think higher or similar based on slope inclinations in Fig.*
368 *4. I do not understand how to estimate the relative contribution of seawater endocytosis and*
369 *transmembrane transport. I guess some trans-membrane ion exchanges (Mg removal) occur*
370 *between seawater vesicles and intrashell cytoplasm. High pCO₂ seawater contains relatively*
371 *large amounts of Zn and Ba ions, which are incorporated into foraminiferal cytoplasm via*
372 *seawater vacuolization. Calcite needles are then precipitated from seawater vesicles with*
373 *modifications by trans-membrane ion exchanges between seawater vesicles and intrashell*
374 *cytoplasm.*

375 **No, high $p\text{CO}_2$ contains the same amount of Zn and Ba ions, only speciation differs.**
376 **Seawater vacuolized at different $p\text{CO}_2$ will have the same Zn and Ba concentration. The**
377 **calcite needles which are precipitated from these vacuoles will have the same Zn/Ca and**
378 **Ba/Ca, unrelated to ambient seawater carbonate chemistry. However, by combining TMT**
379 **and seawater vacuolization, calcification fluid starts with ambient seawater, which is**
380 **diluted with Ca^{2+} by TMT. During this processes, the amount of ions other than Ca^{2+}**
381 **transported to the site of calcification depends on the chemical speciation (amount of free**
382 **ions), the relative abundance compared to Ca^{2+} and the selectivity of and thus**
383 **discrimination by the Ca^{2+} channels. This is now described in more detail in the discussion**
384 **section.**

385

386 **Trends in element incorporation in hyaline and porcelaneous foraminifera as a function of $p\text{CO}_2$**

387 Inge van Dijk¹, Lennart J. de Nooijer¹, Gert-Jan Reichart^{1,2}

388 ¹Department of Ocean Systems, NIOZ-Royal Netherlands Institute for Sea Research, Postbus 59, 1790
389 AB, Den Burg, the Netherlands, and Utrecht University.

390 ²Faculty of Geosciences, Earth Sciences Department, Utrecht University, Budapestlaan 4, 3584 CD,
391 Utrecht, the Netherlands

392

393 **Abstract**

394 In this study we analyzed the impact of seawater carbonate chemistry on the incorporation of elements
395 in both hyaline and porcelaneous larger benthic foraminifera. We observed a higher incorporation of Zn
396 and Ba when $p\text{CO}_2$ increases from 350 to 1200 ppm. Modelling the activity of free ions as a function of
397 $p\text{CO}_2$, shows that speciation of some elements (like Zn and Ba) are mainly influenced by the formation
398 of carbonate complexes in seawater. Hence, differences in foraminiferal uptake of these might be related
399 primarily by the speciation of these elements in seawater. We investigated differences in trends in
400 element incorporation between hyaline (perforate) and porcelaneous (imperforate) foraminifera in order
401 to unravel processes involved in element uptake and subsequent foraminiferal calcification. In hyaline
402 foraminifera we observed a correlation of element incorporation of different elements between species,
403 reflected by a general higher built-in of elements in species with higher Mg content. Between
404 porcelaneous species inter-element differences are much smaller. Besides these contrasting trends in
405 element incorporation, however, similar trends are observed in element incorporation as a function of
406 seawater carbonate chemistry in both hyaline and porcelaneous species. This hints at similar
407 mechanisms responsible for the transportation of ions to the site of calcification for these groups of
408 foraminifera, although the contribution of these processes might differ across species.

409 **1. Introduction**

410 Calcareous foraminifera, cosmopolitan unicellular protists, are widely used to reconstruct past
411 environmental conditions, since the chemical composition of the carbonate shells reflect a wide variety
412 of environmental parameters. For instance, the Mg/Ca of foraminiferal shells is primarily determined
413 by seawater temperature (Nürnberg et al., 1996; Allen and Sanders, 1994) and seawater Mg/Ca (Segev
414 and Erez, 2006; Evans et al., 2015) and has been widely applied as a paleothermometer (Elderfield and
415 Ganssen, 2000; Lear et al., 2000). The use of foraminifera as proxies for the inorganic carbon system in
416 the past (seawater pH, alkalinity, saturation state, etc.) has more recently been added to the foraminiferal
417 proxy tool-box. For example, the concentrations of trace elements in foraminiferal shells, including U
418 (Keul et al., 2013; Russell et al., 2004), Zn (Marchitto et al., 2000; van Dijk et al., 2017) and B (Yu and
419 Elderfield, 2007) correlates to seawater carbonate ion concentration ($[\text{CO}_3^{2-}]$), while the boron isotopic
420 composition of foraminiferal calcite used as a proxy for pH (Sanyal et al., 1996). However, insight in
421 vital effects (Erez, 2003) and inter-specific differences in trace element incorporation (Bentov and Erez,
422 2006; Toyofuku et al., 2011; Wit et al., 2012) is needed to increase robustness of these proxies.

423 On the broadest taxonomic scale foraminifera produce tests using either one of two fundamentally
424 different mechanisms. These calcification strategies reflect the evolutionary separation of foraminiferal
425 groups dating back to the Cambrian diversification, from where the imperforate porcelaneous species
426 and perforate hyaline foraminifera, developed independently (Pawłowski et al., 2003). Previously
427 observed species-specific differences in partitioning and fractionation of elements most likely primarily
428 reflect these differences in calcification strategy, since these offsets are largest between hyaline and
429 porcelaneous species (see for a summary, Toyofuku et al., 2011). The calcification process of the latter
430 group has been studied more extensively than that of the porcelaneous species (De Nooijer et al., 2014).
431 Although many aspects of perforate calcification remain unsolved, there is consensus that chamber
432 formation takes place extracellularly, but within a (semi-) enclosed space, generally termed the site of
433 calcification (SOC). The first layers of calcite precipitate on an organic matrix (the POS or primary
434 organic sheet) that serves as a template for the calcite layer that forms the chamber wall (Erez, 2003;
435 Hemleben et al., 1977). To promote calcification, foraminifera furthermore need to remove Mg ions

436 and/or protons (Zeebe and Sanyal, 2002) from the seawater entering the SOC. A number of larger
437 benthic foraminifera form hyaline shells, although the amount of Mg in their shells is often more than
438 10 times higher than that of planktonic and small benthic hyaline species, hence covering a larger range
439 in Mg/Ca_{CALCITE} values. The calcification strategy of porcelaneous foraminifera is less well studied,
440 which may be partly explained by their limited application in paleoceanography. Porcelaneous
441 foraminifera use a different mode of calcification (Debenay et al., 1998; De Nooijer et al., 2009;
442 Berthold, 1976; Hemleben et al., 1986) and produce shells without pores (hence, the term imperforate)
443 consisting of tablets or needles (Erez, 2003; Bentov and Erez, 2006; Debenay et al., 1998). These calcitic
444 needles (2-3µm) are precipitated intracellularly (Berthold, 1976), after which they are transported out
445 of the foraminifer to form a new chamber (Angell, 1980). At the outer and inner layers of these
446 chambers, the needles are arranged along the same orientation so that they form an optically
447 homogenous surface, giving it a shiny (hence the term ‘porcelaneous’) appearance. In general the Mg/Ca
448 values of the shells of porcelaneous foraminifera are high.

449 Remarkably, despite this large biological control, incorporation of minor and trace elements still reflects
450 environmental conditions, in both hyaline and porcelaneous foraminiferal shells. Systematic offsets
451 between different species, interdependence of trace elements incorporated (Langer et al., 2016) and the
452 different response of element incorporation on element speciation (Wit et al., 2013; Keul et al., 2013;
453 van Dijk et al., 2017), potentially provides useful clues for determining which processes play an
454 important role in the biomineralization pathways. Here we present the results from a controlled growth
455 experiment for which we used several (intermediate- and high-Mg) hyaline and porcelaneous species
456 combined with an inter-species comparison of trace element incorporation. We assessed the impact of
457 bio-calcification on element incorporation as a function of $p\text{CO}_2$ in order to explore the proposed
458 inorganic carbonate proxies (e.g. Zn/Ca; van Dijk et al., 2017) and the impact of different calcification
459 strategies (hyaline versus porcelaneous) on element partitioning. We cultured eight benthic
460 foraminiferal species (4 hyaline and 4 porcelaneous) under four different $p\text{CO}_2$ conditions, analyzing
461 incorporation of Mg, Sr, Na, Zn and Ba.

462

463 **2. Methods**

464 **2.1. Foraminiferal collection**

465 Large samples of macroalgae (*Dictyota* sp.) were collected in November 2015 at a depth of 2-3 meters
466 in Gallows Bay, St. Eustatius (N 17°28'31.6", W62°59'9.4"). Salinity was ~34 and temperature was
467 ~29°C at the site of collection. The collected macroalgae were transported to the laboratory at the
468 Caribbean Netherlands Science Institute (CNSI), where they were placed in a 5 L aquarium with aerated
469 and unfiltered seawater. From this stock, small amounts of algae and debris were gently sieved over a
470 90 and 600 µm mesh to carefully dislodge foraminifera. Several species of foraminifera were picked
471 from the resulting 90-600 µm fraction and directly from the macroalgae. Living specimens of *Sorites*
472 *marginalis* (Lamarck, 1816), *Amphistegina gibbosa* (d'Orbigny, 1839), *Laevipeneroplis bradyi*
473 (Cushman, 1930) and *Archaias angulatus* and limited amounts (<20) of *Peneroplis pertusus* (Forskål,
474 1775), *Asterigerina carinata* (d'Orbigny, 1839), *Heterostegina antillarum* (d'Orbigny, 1839), and
475 *Planorbulina acervalis* (Brady, 1884) characterized by yellow cytoplasm and pseudopodial activity,
476 were selected for the culturing experiments.

477

478 **2.2. Culture set-up**

479 Four barrels, each filled with 100 L of seawater (5µm filtered), were connected to a Li-Cor CO₂/H₂O
480 analyzer (LI-7000), to regulate the CO₂ level in the barrels' head space. The set-points were maintained
481 by addition of CO₂ and/ or CO₂-scrubbed air according to the monitored *p*CO₂. The set-points for *p*CO₂
482 were 350, 450, 760 and 1400 ppm resulting in four batches of seawater (treatment A-D) differing only
483 in their inorganic carbon chemistry. Salinity (34.0±0.2) was monitored with a salinometer (VWR
484 CO310). The fluorescent compound calcein (Bis[N,N-bis(carboxymethyl)aminomethyl]-fluorescein)
485 was added to the culture media (5 mg/L seawater) to enable determination of newly formed chambers
486 during the culture experiment (Bernhard et al., 2004). Short-term exposure (<three weeks) to calcein
487 has no detectable impact on the physiology of benthic foraminifera (Kurtarkar et al., 2015), and the
488 presence of calcein has no effect on the incorporation of Mg and Sr in foraminiferal calcite (Dissard et

489 al., 2009). Culture media was stored air-free in portions of 250 ml in Nalgene bottles with teflon lined
490 caps at 4°C until further use.

491 Foraminifera were divided over the different treatments in duplicate and placed in 70 ml Falcon® tissue
492 bottles with gas-tight caps in a thermostat set at 25°C (Fig. 1). The thermostat was monitored by a
493 temperature logger (Traceable Logger Trac, Maxi Thermal), recording the temperature every minute.
494 The average temperature over the whole experiment was $25 \pm 0.2^\circ\text{C}$. To create uniform light conditions,
495 the thermostat was equipped with two LED shelves, which resulted in high light conditions 12 hr/12hr.
496 Culture media was replaced every four days, to avoid build-up of organic waste and to obtain stable
497 seawater element concentrations and carbon chemistry. Foraminifera were fed after every water change
498 with 0.5 ml of concentrated freeze-dried *Dunaliella salina* cells, pre-diluted with the corresponding
499 treatment seawater. After 21 days, the experiment was terminated. Foraminifera were rinsed three times
500 with de-ionized water, dried at 40°C and stored in micropaleontology slides until further analysis at the
501 Royal Netherlands Institute for Sea Research (NIOZ).

502

503 **2.3. Analytical methods**

504 **2.3.1. Seawater carbon parameters**

505 At the start and termination of the experiment, 125 ml samples of the seawater at each of the different
506 experimental conditions were collected to analyze dissolved inorganic carbon (DIC) and total alkalinity
507 (TA) on a Versatile INstrument for the Determination of Titration Alkalinity (VINDTA) at the CNSI.
508 Using the measured DIC and TA values and the software CO2SYS v2.1, adapted to Excel by Pierrot et
509 al. (2006) the other carbon parameters (including $[\text{CO}_3^{2-}]$ and Ω_{CALCITE}) were calculated. For this we
510 used the equilibrium constants for K1 and K2 from Lueker et al. (2000) and KHSO_4 from (Dickson,
511 1990) (Table 1).

512

513 **2.3.2. Seawater element concentrations**

514 At the start and end of the experiment and during replacement of the culture media, subsamples were
515 collected in duplo using 50 ml LDPE Nalgene bottles and immediately frozen at -80°C . After
516 transportation to the NIOZ, defrosted samples were acidified with 3 times Quartz distilled HCl to pH
517 ~ 1.8 and the seawater composition of the samples was analyzed on an Element 2 sector field double
518 focusing mass spectrometer (SF-ICP-MS) run in medium resolution mode. IAPSO (International
519 Association for the Physical Sciences of the Ocean) Standard Seawater was used as a drift monitor.
520 Analytical precision (relative standard deviation) was 3% for Ca, 4% for Mg, 1% Na, 1% for Sr and 5%
521 Ba. We obtained average values of 5.25 ± 0.06 mol/mol for Mg/Ca, 44.6 ± 0.6 mol/mol for Na/Ca,
522 8.63 ± 0.05 mol/mol for Sr/Ca, and 9.04 ± 0.47 $\mu\text{mol/mol}$ for Ba/Ca.

523 A subsample was analyzed using a commercially available pre-concentration system, SeaFAST S2.
524 With the SeaFAST system elements with low concentrations are pre-concentrated to values above
525 detection limit of the SF-ICP-MS. Accordingly, we measured Cd, Pb U, B, Ti, Mn, Fe, Co, Ni, Cu, and
526 Zn. In short, 10ml of sample was mixed with an ammonium acetate buffer to pH 6.2 and loaded on a
527 column containing NOBIAS chelating agent. After rinsing the column with a diluted ammonium acetate
528 buffer the metals were eluted in 750 μl of quartz distilled 1.5 M HNO_3 before being quantified on the
529 SF-ICP-MS. Here we use the Zn data only, as this was analyzed in the foraminifera as well. Analytical
530 precision (relative standard deviation) was 5% for Zn. We obtained an average value of 15.3 ± 0.5
531 $\mu\text{mol/mol}$ for seawater Zn/Ca for all treatments. Although these values are clearly above natural open
532 ocean values, the concentrations are very uniform between treatments and when comparing start and
533 end of the experiments. The contamination with Zn might hence have occurred already when filling the
534 culture setup with the waters from the bay adjacent to the culture facility. Concentrations are well below
535 values considered harmful for foraminifera (Nardelli et al., 2016).

536

537 **2.3.3. Cleaning methods**

538 After termination of the experiment, foraminiferal shells were cleaned following an adapted version of
539 Barker et al. (2003). Per treatment duplicate, all foraminifera were transferred to 10 ml polyethylene

540 vials. To each vial, 10 mL 1% H₂O₂ solution (buffered with 0.5M NH₄OH) was added to remove organic
541 matter. The vials were heated for 10 minutes in a water bath at 95 °C, and placed in an ultrasonic bath
542 for 30 seconds (degas mode, 80kHz, 50% power), after which the oxidizing reagent was removed. These
543 steps (organic removal procedure) were repeated five times. Foraminiferal samples were rinsed five
544 times with ultrapure water, after which the vials were stored overnight in a laminar flow cabinet at room
545 temperature to dry. Dried foraminifera were placed on double sided tape on LA-ICP-MS stubs. Pictures
546 were taken of individual foraminifera with a ZEISS Axioplan 2 fluorescence microscope equipped with
547 appropriate excitation and emission optics and a ZEISS Axiocam MRc 5 camera, to assess the number
548 of chambers added during the experiment based on the incorporation of calcein.

549

550 **2.3.4. LA-ICP-MS**

551 Element concentrations of individual fluorescent chambers were analyzed by Laser Ablation-ICP-MS
552 (Reichert et al., 2003; van Dijk et al., 2017). To determine foraminiferal element concentrations, the
553 laser system (NWR193UC, New Wave Research) at the Royal NIOZ was equipped with a Two Volume
554 2 cell (New Wave Research), characterized by a wash-out time of 1.8 seconds (1% level) and hence
555 allowing detection of variability of obtained element to Ca ratios within chamber walls. Single chambers
556 were ablated in a helium environment using a circular laser spot with a diameter of 80 µm (*S. marginalis*)
557 or 60 µm (other species). We ablated all calcein-stained chambers twice, except for the first 1-2
558 chambers that formed during the experiment to avoid contamination of calcite of chambers formed prior
559 to the experiments and overlapped by the labelled chambers (Fig.2).

560 All foraminiferal samples were ablated with an energy density of 1±0.1 J/cm² and a repetition rate of 6
561 Hz. The resulting aerosol was transported on a helium flow through an in house build smoothing device,
562 being mixed with a nitrogen flow (5 ml/min), before entering the quadrupole ICP-MS (iCAP-Q, Thermo
563 Scientific). Monitored masses included ⁷Li, ¹¹B, ²³Na, ²⁴Mg, ²⁵Mg, ²⁷Al, ⁴³Ca, ⁴⁴Ca, ⁶⁶Zn, ⁸⁸Sr and ¹³⁷Ba.
564 Contrary to ⁶⁷Zn and ⁶⁸Zn, ⁶⁶Zn is free of interferences when measuring calcium carbonate and SRM
565 NIST (National Institute of Standard and Technology, U.S., Standard Reference Material) glass

566 standards (Jochum et al., 2012). Potential contamination or diagenesis of the outer or inner layer of
567 calcite was excluded by monitoring the Al signal. At the start of each series, we analyzed SRM NIST612
568 and NIST610 glass standard in triplicate (using an energy density of $5 \pm 0.1 \text{ J/cm}^2$), JcT-1 (coral
569 carbonate) and two in-house standards, namely NFHS (NIOZ Foraminifera House Standard; Mezger et
570 al., 2016) and the Iceland spar NCHS (NIOZ Calcite House Standard). We further analyzed JcP-1 (coral,
571 *Porites* sp.; Okai et al., 2002) and MACS-3 (Synthetic Calcium Carbonate) at the start of each series,
572 and to monitor drift after every ten samples. All element to calcium ratios were calculated with an
573 adapted version of the MATLAB based program SILLS (Signal Integration for Laboratory Laser
574 Systems; Guillong et al., 2008). SILLS was modified by NIOZ to evaluate LA-ICP-MS measurements
575 on foraminifera, allowing import of Thermo Qtegra software sample list, laser data reduction and laser
576 LOG files. Major adaptations include improved automated integration and evaluation of (calibration and
577 monitor) standards, quality control report of the monitor standards and export in element to calcium
578 ratios (mmol/mol). Calibration was performed against the MACS-3 carbonate standard, with ^{43}Ca as an
579 internal standard and we used the multiple measurements of MACS-3 for a linear drift correction.
580 Relative analytical precision (relative standard deviation (RSD) of all MACS-3 analyses) is 3% for ^{23}Na ,
581 3% for ^{24}Mg , 3% for ^{25}Mg , 4% for ^{66}Zn , 3% for ^{88}Sr and 3% for ^{137}Ba . In total, 961 analyses were
582 performed on 251 specimens covering eight species cultured in four experimental conditions (see Table
583 2 for details).

584 We calculated the standard deviation (SD), RSD and standard error (SD/\sqrt{n} ; SE) per treatment. The
585 partitioning coefficient (D) of an element (E) between seawater and foraminiferal calcite is expressed
586 as $D_E = (E/\text{Ca}_{\text{CALCITE}})/(E/\text{Ca}_{\text{SW}})$. Partition coefficients and element versus calcium ratio were statistically
587 compared with different experimental parameters (such as $p\text{CO}_2$ or $[\text{CO}_3^{2-}]$) using a two-sided t-test with
588 95% confidence levels. This also allows for the calculation of 95% confidence intervals over the average
589 per treatment. Pairwise comparisons were made for per E/Ca per species and culture conditions using
590 ANOVA. Groups that showed significant difference were assigned different letters. When comparing
591 partition coefficients to other studies, E/Ca_{SW} data was, in some studies, not measured. For these studies

592 we used average seawater E/Ca_{SW} to calculate D_E (see also supplementary Table 1), allowing
593 comparing partitioning coefficients.

594

595 **3. Results**

596 **3.1. Element/Ca as a function of ocean acidification**

597 In hyaline species $Mg/Ca_{CALCITE}$ varies between 25.9-141.3 mmol/mol Mg/Ca . In contrast, $Mg/Ca_{CALCITE}$
598 of porcelaneous species ranges from 121.3-149.3 mmol/mol (Table 3). This large spread in foraminifera
599 E/Ca of hyaline species is also observed for Sr (1.7-3.1 mmol/mol), Na (3.4-19.5 mmol/mol), Zn (9.0-
600 97.0 $\mu\text{mol/mol}$) and Ba (2.7-20.1 $\mu\text{mol/mol}$), while porcelaneous species only vary over a narrow range
601 (Sr = 2.0-2.2 mmol/mol; Na = 3.8-5.8 mmol/mol; Zn = 53.0-140.8 $\mu\text{mol/mol}$; Ba = 18.0-29.0 $\mu\text{mol/mol}$).

602 In both porcelaneous and hyaline species we find an increase of $Zn/Ca_{CALCITE}$ and $Ba/Ca_{CALCITE}$ with
603 pCO_2 , while foraminiferal Sr/Ca, Mg/Ca and Na/Ca remain similar across the experimental conditions
604 (Fig. 3 and Table 4). Sensitivity of both foraminiferal Zn/Ca and Ba/Ca to changes in seawater pCO_2
605 differs between the studied porcelaneous and hyaline species. When pCO_2 changes from 350 to 1200
606 ppm, Zn/Ca of hyaline foraminifera increase by a factor of 3.7 (*A. carinata*) or 4.5 (*A. gibbosa*) while
607 porcelaneous foraminiferal Zn/Ca increases only by 1.3 (*S. marginalis*), 1.8 (*A. angulatus*) and 2.1 (*L.*
608 *bradyi*). Also sensitivity of foraminiferal Ba/Ca to the same change in pCO_2 shows a similar pattern,
609 with Ba/Ca of hyaline species increasing by a factor of 3.6 (*A. carinata*) or 3.7 (*A. gibbosa*), while
610 porcelaneous species increase Ba/Ca only with a factor of 1.8 (*S. marginalis*), 1.6 (*A. angulatus*) or 2.1
611 (*L. bradyi*).

612

613 **3.2. Inter-species differences in element incorporation**

614 When comparing Mg incorporation to that of the other elements studied here (Ba, Zn, Sr and Na)
615 between hyaline species (treatment B; Table 3), we observe a positive relation between D_{Mg} with D_{Sr}
616 ($p < 0.0025$), D_{Na} ($p < 0.0005$), D_{Ba} ($p < 0.05$) and D_{Zn} ($p < 0.005$). In general hyaline species are enriched

617 similarly in all elements (Fig. 4). Compared to porcelaneous species, the hyaline shell building species
618 which incorporate most Mg (>100 mmol/mol Mg/Ca) incorporate more Na, and Sr, while incorporating
619 less Zn and Ba. Element incorporation across porcelaneous species is less variable than observed for
620 hyaline species. Including data from literature (both culture and field calibrations; see supplementary
621 Table S1), preferable in which both Mg/Ca and at least one other element (Na, Sr, Ba or Zn) is measured,
622 shows that the relation based on the Caribbean species studied here is also more general applicable when
623 including more species ($D_{Sr} = p < 0.005$; $D_{Na} = p < 0.0005$; $D_{Ba} = p < 0.005$; $D_{Zn} = p < 0.01$), even though
624 this compiled data (labeled 'All studies' in Tabel S2) covers a somewhat wider range in environmental
625 and experiment conditions.

626

627 **4. Discussion**

628 **4.1. Effect of ocean acidification on Element/Ca**

629 For neither porcelaneous nor hyaline species, foraminiferal Mg/Ca, Na/Ca and Sr/Ca systematically
630 change with pCO_2 . The impact of pH (and/or $[CO_3^{2-}]$) on $Mg/Ca_{CALCITE}$ and $Sr/Ca_{CALCITE}$ in foraminifera
631 has been the subject of discussion (e.g., Dissard et al., 2010; Elderfield et al., 1996). In deep-sea benthic
632 species, incorporation of certain elements is governed by carbonate system as observed for Zn by
633 Marchitto et al. (2005) and Cd and Ba by McCorkle et al. (1995). Observed response to changes in
634 carbonation ion concentration are in these studies mainly due to calcification in undersaturated seawater,
635 as described by 'the carbonate ion saturation hypothesis' (Elderfield et al., 2006). In some low-Mg
636 benthic species, both $Mg/Ca_{CALCITE}$ and $Sr/Ca_{CALCITE}$ do not seem to depend on inorganic carbon system
637 parameters, e.g. pH or $[CO_3^{2-}]$ (Allison et al., 2011; Dueñas-Bohórquez et al., 2011). However, for
638 several planktonic species pH does influence $Mg/Ca_{CALCITE}$ and $Sr/Ca_{CALCITE}$ (Russell et al., 2004; Lea
639 et al., 1999; Evans et al., 2016). The effect of pH on $Sr/Ca_{CALCITE}$ might be explained via increased
640 growth rates due to pH-associated changes in $[CO_3^{2-}]$ (Dissard et al., 2010). However, due to the limited
641 experimental set-up, we are not able to disentangle the effects of the different carbon parameters in this
642 study. Still, here we show that incorporation of Mg, Sr and Na of the selected larger benthic hyaline and

643 porcelaneous foraminifera are not significantly impacted when cultured over a limited range of $p\text{CO}_2$
644 and thus $[\text{CO}_3^{2-}]$ and pH values.

645 In contrast, foraminiferal Zn/Ca and Ba/Ca are significantly impacted by $p\text{CO}_2$ for all species studied
646 here (Table 4; Fig. 3). Although Hönisch et al. (2011) suggested that the impact of carbonate chemistry
647 on Ba incorporation is negligible, their data does suggest a trend over the same interval in pH as studied
648 here. In hyaline foraminifera, Zn/Ca and Ba/Ca increases more as a function of $p\text{CO}_2$ (factor of 3.7-4.5
649 and 3.6-3.7, respectively when $p\text{CO}_2$ increases from 350 to 1200 ppm) compared to the porcelaneous
650 species (1.3-2.1 and 1.6-2.1 times, respectively). This observation suggests that the mechanisms
651 involved in uptake of Ba and Zn are similar for porcelaneous and hyaline species, although the
652 contribution of this process is different, which leads to differences in the sensitivity of Zn and Ba
653 incorporation with $p\text{CO}_2$

654

655 **4.2. Speciation in the microenvironment**

656 In the culture set-up used, increasing $p\text{CO}_2$ increases DIC, reduces pH and thereby decreases seawater
657 $[\text{CO}_3^{2-}]$. Speciation of Zn, Ba and also other elements, like U (Keul et al., 2013; Russell et al., 2004; van
658 Dijk et al., 2017), is primarily controlled by seawater $[\text{CO}_3^{2-}]$. The speciation of all elements studied
659 here (Mg, Na, Sr, Zn and Ba) for our different seawater treatments were modelled using PHREEQC, a
660 computer program for speciation, batch-reaction, one-dimensional transport, and inverse geochemical
661 calculations (Parkhurst and Appelo, 1999). For this we used the standard in-software Ilnl database, a
662 PHREEQC database that implements most of the inorganic aqueous species and minerals in the
663 thermodynamic data and includes many elements not available in any other PHREEQC database. We
664 observed a decrease of free ions (Zn^{2+} and Ba^{2+}) and an increase in Ba and Zn carbonate complexes
665 (BaCO_3^0 and ZnCO_3^0), with increasing $p\text{CO}_2$ (Fig. 5), while the activity of Mg^{2+} , Na^+ and Sr^{2+} remained
666 similar. This suggests that element incorporation in foraminiferal calcite might be depending on the
667 availability of free ions, which in the case of Ba and Zn, changes with $p\text{CO}_2$. This is contrary to inorganic

668 precipitation, were carbonate complexes (e.g. MgCO_3^0) are easily incorporated into the calcite crystal
669 lattice.

670

671 **4.3. Trends in element incorporation**

672 Element incorporation in hyaline foraminifera is highly interdependent, i.e. species with increased Mg
673 content also incorporate more Sr, Na, Ba and Zn (Fig. 3). The linear increase in Sr incorporation with
674 increasing Mg/Ca has also been observed for other hyaline species, like *Operculina ammonoides* (Evans
675 et al., 2015), *Amphistegina lessonii* and *Ammonia aomoriensis* (Mewes et al., 2015), which both fall on
676 the same trend as that for inorganic calcite (Mucci and Morse, 1983). Evans et al. (2015) hypothesize
677 that the incorporation of other alkali elements, like Na is also related, due to lattice distortion by the
678 incorporation of Mg, which has been found in inorganic calcite (Okumura and Kitano, 1986). However,
679 although this mechanism might explain some of the observed species specific element incorporation in
680 hyaline foraminifera, this does not explain the observed difference between hyaline and porcelaneous
681 foraminifera (Figure 4). Porcelaneous foraminifera have generally high Mg/Ca, but we actually observe
682 lower incorporation of Na and Sr compared to hyaline species with similar D_{Mg} (Fig 4, upper right and
683 left panel: D_{Mg} versus D_{Na} and D_{Sr}). When including porcelaneous species from other studies we also
684 observe no increase in D_{Sr} over a larger range in D_{Mg} (Fig S1, upper left panel: D_{Mg} versus D_{Sr}).
685 Therefore, even though this interdependence might partly stem from mechanisms associated with
686 crystallography, differences between hyaline and porcelaneous foraminifera suggest it could also be
687 caused by mechanisms involved in take up the ions (Ca^{2+} and CO_3^{2-}) necessary for chamber formation,
688 which are different for hyaline and porcelaneous species, reflected in the different trends observed here.

689

690 **4.4. Ion transport models**

691 Both porcelaneous and hyaline foraminifera promote calcification by increasing their internal pH (De
692 Nooijer et al., 2009). Still, they might use different mechanisms to take up the ions (Ca^{2+} and CO_3^{2-})

693 necessary for chamber formation, which is reflected in the different trends observed here. In both
694 porcelaneous and hyaline foraminifera, E/Ca respond similarly to changes in $p\text{CO}_2$ (Fig 3), suggesting
695 uptake of all these elements is controlled by the same process. However, we observed different inter-
696 element relations between hyaline and porcelaneous foraminifera (Fig. 4), indicating the mechanisms
697 for ion transport might be different for these two groups. Two of the main concepts of ion transport in
698 foraminifera are transmembrane transport (Nehrke et al., 2013) and the inclusion of seawater by
699 seawater endocytosis (Bentov et al., 2009). Here we try to validate these two concept by comparing
700 them with our observations.

701

702 **4.4.1. Transmembrane transport**

703 During calcification, Ca^{2+} is proposed to be transported from seawater to the SOC via ion channels
704 (Nehrke et al., 2013), likely in exchange for protons (Toyofuku et al., accepted). This so-called trans-
705 membrane transport (TMT) through Ca^{2+} channels has also been found for other marine organisms,
706 including coccolithophores (Gussone et al., 2006). These Ca^{2+} channels may not discriminate perfectly
707 between Ca ions and elements like Mg, Sr, Ba, Na (Sather, 2005; Allen and Sanders, 1994; Hess and
708 Tsien, 1984), causing accidental transport of these elements into the SOC. How much of a certain
709 element will enter the SOC in this way, depends on 1) the selectiveness of the channels and the
710 characteristics of the transported ions (like atomic radius), 2) the element to calcium ratio in the
711 foraminiferal microenvironment and 3) the concentration gradient between seawater and the SOC. The
712 availability of some free ions, like Ba and Zn, changes as a function of $p\text{CO}_2$ due to the formation of
713 carbonate complexes (Fig. 5). When Zn and Ba form stable complexes with carbonate ions they are no
714 longer available for (sporadic) transport through the Ca^{2+} channels, decreasing the availability at the site
715 of calcification and subsequently, incorporation into the foraminiferal calcite. Thus, transmembrane
716 transport of ions by Ca^{2+} to the SOC is in agreement with our results (Fig. 3). The amount of Zn and Ba
717 available at the site of calcification is proportional to the concentration of the ratio between Ca^{2+} and
718 free Zn^{2+} and Ba^{2+} in the foraminiferal microenvironment. In turn, the amount of free Zn and Ba ions in
719 seawater is controlled by their respective concentration in seawater concentration, as well as carbonate

720 chemistry (Fig 5). Foraminiferal Mg/Ca, Na/Ca and Sr/Ca is not detectably affected, since the
721 availability of Mg^{2+} , Na^+ and Sr^{2+} does not change over the range of $[CO_3^{2-}]$ studied here. However, the
722 large range in Mg/Ca values in hyaline species suggests that TMT might play a variable role in the
723 calcification process of these species. This may result in an interdependence between all these elements
724 studied such as observed here for the hyaline species if the selectivity for Ca^{2+} of these channels varies
725 between species.

726

727 **4.4.2. Seawater endocytosis**

728 Another proposed ion transport mechanism is seawater endocytosis (Bentov et al., 2009; Erez, 2003),
729 in which seawater is vacuolized, altered and then used as a calcifying fluid. The chemistry or elemental
730 composition of the vacuolized seawater or the calcification fluid is in this case depending on the seawater
731 concentration. Inter-species differences would therefore be minimized, as is observed for porcelaneous
732 foraminifera in our study (Fig. 4). However, this concept cannot explain the overserved changes in
733 Zn/Ca and Ba/Ca as a function of pCO_2 , which are caused by the speciation of elements in seawater due
734 to changes in the carbonate chemistry (Fig. 5). The concentration of total e.g. Zn in the seawater vacuoles
735 does not change for the different treatments, only the species of Zn present. Only if the internal pH in
736 the vacuole depends on ambient seawater pH, which is currently unknown, there is a potential for
737 changes in speciation. In theory, if pH will change in concert with ambient seawater, such a change in
738 internal pH from >9 (De Nooijer et al., 2009) to >8.6 ($\Delta pH = 0.4$ in our treatment) changes $[CO_3^{2-}]$ and
739 thus the speciation of e.g. Zn (and Ba) at the site of calcification. However, over this range the change
740 in $[CO_3^{2-}]$ will be rather limited and hence such an effect of differential speciation within the calcifying
741 fluid does not suffice to explain the observed sensitivity of Zn and Ba to pCO_2 in our study. This is in
742 line with recent evidence on Zn/Ca in foraminifera, which suggests Zn incorporation is not primarily
743 governed by changes in seawater pH, but by carbonate ion concentration, which does not change much
744 at these high pH's (van Dijk et al., 2017).

745

746 **4.5. Consequences for calcification in hyaline and porcelaneous species**

747 Both ion transport mechanisms, and their consequences for Zn and Ba incorporation, are summarized
748 in Fig. 6. The observed species-specific element incorporation in hyaline foraminifera (Fig. 4) is
749 compatible with the transmembrane transport mixing model proposed by Nehrke et al. (2013), where
750 species specific differences in E/Ca are explain by the relative contribution of transmembrane transport
751 and so-called passive transport. In contrast to hyaline species, the porcelaneous species show much less
752 inter-species variation in element composition (Fig. 3), suggesting that this group of foraminifera calcify
753 from a fluid comparable to ambient seawater (Ter Kuile and Erez, 1987), by e.g. seawater endocytosis
754 (Fig. 6, panel B) with only minor alteration of the elemental composition of the calcifying fluid by ion
755 channels. However, the observed correlation between $p\text{CO}_2$ and Ba and Zn (Fig. 3) suggests that Ca
756 channels still play a (modest) role in supplying Ca^{2+} to the porcelaneous SOC, since possible speciation
757 of minor and trace elements in the SOC caused by a change in the internal pH is probably not sufficient
758 to explain observed patterns (4.4.2). However since porcelaneous species already obtain calcium by
759 including seawater in their calcification vesicle prior to calcite precipitation, contribution of Ca^{2+}
760 through TMT is likely smaller than in hyaline species, which may explain the observed lower sensitivity
761 of e.g. foraminiferal Zn/Ca and Ba/Ca to changes in seawater $[\text{CO}_3^{2-}]$ in porcelaneous species (Fig. 3).
762 This approximately 2 times lower sensitivity of porcelaneous foraminifera compared to hyaline species
763 suggests that porcelaneous foraminifera acquire half of the necessary Ca^{2+} through Ca-channels
764 compared to hyaline species. Element incorporation in porcelaneous foraminifera will therefore be
765 mainly governed by their respective concentrations in seawater, and to a lesser extent by the selectivity
766 for Ca^{2+} /permeability for other ions during TMT.

767

768 **5. Conclusions**

769 Trends in element incorporation in larger benthic foraminifera can be explained by a combination of
770 differences in calcification strategy and seawater chemistry. Carbonate chemistry of seawater
771 determines speciation and therefore availability of some ions (e.g. Zn^{2+} and Ba^{2+}), which are available

772 for ion transport to the site of calcification. For hyaline foraminifera, we observed species-specific
773 interdependence of element incorporation, which can be explained by a previously proposed
774 transmembrane transport model and the bioavailability of ions in seawater during calcification. For
775 porcelaneous foraminifera, species specific difference are small, hinting at a higher contribution of
776 another ion source, like e.g. seawater endocytosis.

777

778 **Acknowledgments**

779 This research is funded by the NIOZ – Royal Netherlands Institute for Sea Research and the Darwin
780 Centre for Biogeosciences project “*Double Trouble: Consequences of Ocean Acidification – Past,*
781 *Present and Future –Evolutionary changes in calcification mechanisms*” and the program of the
782 Netherlands Earth System Science Center (NESSC). We would like to thanks both reviewers, Dr. David
783 Evans and Dr. Kazuhiko Fujita for their constructive comments. Great thanks to Johan Stapel for hosting
784 the 2015 foraminifera culture expedition at the CNSI, St. Eustatius, as well as all the participants: Jelle
785 Bijma and Gernot Nehrke (AWI), Brett Metcalfe (VU), Alice Webb (NIOZ), Esmee Geerken (NIOZ)
786 and Didier de Bakker (NIOZ/IMARES). This study would not have been possible without Steven van
787 Heuven and Bob Koster, who designed and constructed the $p\text{CO}_2$ set-up (NWO grants 858.14.021 and
788 858.14.022). Furthermore, we would like to thank Kirsten Kooijman for supplying *Dunaliella salina*
789 cultures, Patrick Laan and Karel Bakker for seawater analysis and Mariëtte Wolthers for providing
790 technical support with PHREEQC. Lastly, we thank Jan-Berend Stuut (NIOZ) for the usage of the
791 Hitachi TM3000 SEM (NWO grant 822.01.008 and ERC grant 311152).

792 **References**

793 Allen, G. J., and Sanders, D.: Two Voltage-Gated, Calcium Release Channels Coreside in
794 the Vacuolar Membrane of Broad Bean Guard Cells, *The Plant Cell*, 6, 685-694,
795 10.1105/tpc.6.5.685, 1994.

796 Allison, N., Austin, H., Austin, W., and Paterson, D. M.: Effects of seawater pH and
797 calcification rate on test Mg/Ca and Sr/Ca in cultured individuals of the benthic, calcitic
798 foraminifera *Elphidium williamsoni*, *Chemical Geology*, 289, 171-178,
799 10.1016/j.chemgeo.2011.08.001, 2011.

800 Angell, R. W.: Test morphogenesis (chamber formation) in the foraminifer *Spiroloculina*
801 *hyalina* Schulze, *Journal of Foraminiferal Research*, 10, 89-101, 1980.

802 Barker, S., Higgins, J. A., and Elderfield, H.: The future of the carbon cycle: review,
803 calcification response, ballast and feedback on atmospheric CO₂, *Philos Trans A Math Phys*
804 *Eng Sci*, 361, 1977-1998; discussion 1998-1979, 10.1098/rsta.2003.1238, 2003.

805 Bentov, S., and Erez, J.: Impact of biomineralization processes on the Mg content of
806 foraminiferal shells: A biological perspective, *Geochemistry, Geophysics, Geosystems*, 7,
807 2006.

808 Bentov, S., Brownlee, C., and Erez, J.: The role of seawater endocytosis in the
809 biomineralization process in calcareous foraminifera, *Proceedings of the National Academy of*
810 *Sciences of the United States of America*, 106, 21500-21504, 10.1073/pnas.0906636106, 2009.

811 Bernhard, J. M., Blanks, J. K., Hintz, C. J., and Chandler, G. T.: Use of the fluorescent calcite
812 marker calcein to label foraminiferal tests, *Journal of Foraminiferal Research*, 34, 96-101,
813 10.2113/0340096, 2004.

814 Berthold, W.-U.: Biomineralisation bei milioliden Foraminiferen und die Matritzen-
815 Hypothese, *Naturwissenschaften*, 63, 196-197, 1976.

816 De Nooijer, L. J., Toyofuku, T., and Kitazato, H.: Foraminifera promote calcification by
817 elevating their intracellular pH, *Proceedings of the National Academy of Sciences*, 106, 15374-
818 15378, [10.1073/pnas.0904306106](https://doi.org/10.1073/pnas.0904306106), 2009.

819 De Nooijer, L. J., Spero, H. J., Erez, J., Bijma, J., and Reichart, G. J.: Biomineralization in
820 perforate foraminifera, *Earth-Science Reviews*, 135, 48-58,
821 [http://dx.doi.org/10.1016/j.earscirev.2014.03.013](https://dx.doi.org/10.1016/j.earscirev.2014.03.013), 2014.

822 Debenay, J.-P., Guillou, J.-J., Geslin, E., Lesourd, M., and Redois, F.: Processus de
823 cristallisation de plaquettes rhomboédriques à la surface d'un test porcelané de foraminifère
824 actuel, *Geobios*, 31, 295-302, 1998.

825 Dickson, A. G.: Thermodynamics of the dissociation of boric acid in synthetic seawater from
826 273.15 to 318.15 K, *Deep Sea Research Part A. Oceanographic Research Papers*, 37, 755-766,
827 [http://dx.doi.org/10.1016/0198-0149\(90\)90004-F](https://dx.doi.org/10.1016/0198-0149(90)90004-F), 1990.

828 Dissard, D., Nehrke, G., Reichart, G. J., Nouet, J., and Bijma, J.: Effect of the fluorescent
829 indicator calcein on Mg and Sr incorporation into foraminiferal calcite, *Geochemistry,*
830 *Geophysics, Geosystems*, 10, [10.1029/2009GC002417](https://doi.org/10.1029/2009GC002417), 2009.

831 Dissard, D., Nehrke, G., Reichart, G. J., and Bijma, J.: Impact of seawater $p\text{CO}_2$ on
832 calcification and Mg/Ca and Sr/Ca ratios in benthic foraminifera calcite: results from culturing
833 experiments with *Ammonia tepida*, *Biogeosciences*, 7, 81-93, [10.5194/bg-7-81-2010](https://doi.org/10.5194/bg-7-81-2010), 2010.

834 Dueñas-Bohórquez, A., Raitzsch, M., De Nooijer, L. J., and Reichart, G.-J.: Independent
835 impacts of calcium and carbonate ion concentration on Mg and Sr incorporation in cultured
836 benthic foraminifera, *Marine Micropaleontology*, 81, 122-130,
837 [10.1016/j.marmicro.2011.08.002](https://doi.org/10.1016/j.marmicro.2011.08.002), 2011.

838 Elderfield, H., Bertram, C. J., and Erez, J.: A biomineralization model for the incorporation
839 of trace elements into foraminiferal calcium carbonate, *Earth and Planetary Science Letters*,
840 142, 409-423, [http://dx.doi.org/10.1016/0012-821X\(96\)00105-7](https://dx.doi.org/10.1016/0012-821X(96)00105-7), 1996.

841 Elderfield, H., and Ganssen, G.: Past temperature and $\delta^{18}\text{O}$ of surface ocean waters inferred
842 from foraminiferal Mg/Ca ratios, *Nature*, 405, 442-445, 2000.

843 Elderfield, H., Yu, J., Anand, P., Kiefer, T., and Nyland, B.: Calibrations for benthic
844 foraminiferal Mg/Ca paleothermometry and the carbonate ion hypothesis, *Earth and Planetary*
845 *Science Letters*, 250, 633-649, 2006.

846 Erez, J.: The source of ions for biomineralization in foraminifera and their implications for
847 paleoceanographic proxies, *Reviews in Mineralogy and Geochemistry*, 54, 115-149,
848 10.2113/0540115, 2003.

849 Evans, D., Erez, J., Oron, S., and Müller, W.: Mg/Ca-temperature and seawater-test
850 chemistry relationships in the shallow-dwelling large benthic foraminifera *Operculina*
851 *ammonoides*, *Geochimica et Cosmochimica Acta*, 148, 325-342, 2015.

852 Evans, D., Wade, B. S., Henehan, M., Erez, J., and Müller, W.: Revisiting carbonate
853 chemistry controls on planktic foraminifera Mg/Ca: implications for sea surface temperature
854 and hydrology shifts over the Paleocene–Eocene Thermal Maximum and Eocene–Oligocene
855 transition, *Clim. Past*, 12, 819-835, 10.5194/cp-12-819-2016, 2016.

856 Guillong, M., Meier, D. L., Allan, M. M., Heinrich, C. A., and Yardley, B. W.: SILLS: A
857 MATLAB-based program for the reduction of laser ablation ICP-MS data of homogeneous
858 materials and inclusions, *Mineralogical Association of Canada Short Course Series*, 40, 328-
859 333, 2008.

860 Gussone, N., Langer, G., Thoms, S., Nehrke, G., Eisenhauer, A., Riebesell, U., and Wefer,
861 G.: Cellular calcium pathways and isotope fractionation in *Emiliana huxleyi*, *Geology*, 34, 625-
862 628, 2006.

863 Hemleben, C., Be, A. W. H., Anderson, O. R., and Tuntivate, S.: Test morphology, organic
864 layers and chamber formation of the planktonic foraminifer *Globorotalia menardii* (d'Orbigny),
865 *Journal of Foraminiferal Research*, 7, 1-25, 10.2113/gsjfr.7.1.1, 1977.

866 Hemleben, C., Erson, O., Berthold, W., and Spindler, M.: fout, Biomineralization in lower
867 plants and animals (BSC Leadbeater, R Riding, eds) Clarendon Press, Oxford, 237-249, 1986.

868 Hess, P., and Tsien, R. W.: Mechanism of ion permeation through calcium channels, Nature,
869 309, 453-456, 1984.

870 Hönisch, B., Allen, K. A., Russell, A. D., Eggins, S. M., Bijma, J., Spero, H. J., Lea, D. W.,
871 and Yu, J.: Planktic foraminifers as recorders of seawater Ba/Ca, Marine Micropaleontology,
872 79, 52-57, 2011.

873 Jochum, K. P., Scholz, D., Stoll, B., Weis, U., Wilson, S. A., Yang, Q., Schwab, A., Börner,
874 N., Jacob, D. E., and Andreae, M. O.: Accurate trace element analysis of speleothems and
875 biogenic calcium carbonates by LA-ICP-MS, Chemical Geology, 318–319, 31-44,
876 <http://dx.doi.org/10.1016/j.chemgeo.2012.05.009>, 2012.

877 Keul, N., Langer, G., De Nooijer, L. J., Nehrke, G., Reichart, G.-J., and Bijma, J.:
878 Incorporation of uranium in benthic foraminiferal calcite reflects seawater carbonate ion
879 concentration, Geochemistry, Geophysics, Geosystems, 14, 102-111, 10.1029/2012gc004330,
880 2013.

881 Kurtarkar, S. R., Saraswat, R., Nigam, R., Banerjee, B., Mallick, R., Naik, D. K., and Singh,
882 D. P.: Assessing the effect of calcein incorporation on physiological processes of benthic
883 foraminifera, Marine Micropaleontology, 114, 36-45,
884 <http://dx.doi.org/10.1016/j.marmicro.2014.10.001>, 2015.

885 Langer, G., Sadekov, A., Thoms, S., Keul, N., Nehrke, G., Mewes, A., Greaves, M., Misra,
886 S., Reichart, G.-J., de Nooijer, L. J., Bijma, J., and Elderfield, H.: Sr partitioning in the benthic
887 foraminifera *Ammonia aomoriensis* and *Amphistegina lessonii*, Chemical Geology, 440, 306-
888 312, <http://dx.doi.org/10.1016/j.chemgeo.2016.07.018>, 2016.

889 Lea, D. W., Mashiotta, T. A., and Spero, H. J.: Controls on magnesium and strontium uptake
890 in planktonic foraminifera determined by live culturing, *Geochimica et Cosmochimica Acta*,
891 63, 2369-2379, [http://dx.doi.org/10.1016/S0016-7037\(99\)00197-0](http://dx.doi.org/10.1016/S0016-7037(99)00197-0), 1999.

892 Lear, C. H., Elderfield, H., and Wilson, P. A.: Cenozoic deep-Sea temperatures and global
893 ice volumes from Mg/Ca in benthic foraminiferal calcite, *Science*, 287, 269-272,
894 10.1126/science.287.5451.269, 2000.

895 Lueker, T. J., Dickson, A. G., and Keeling, C. D.: Ocean pCO₂ calculated from dissolved
896 inorganic carbon, alkalinity, and equations for K₁ and K₂: validation based on laboratory
897 measurements of CO₂ in gas and seawater at equilibrium, *Marine Chemistry*, 70, 105-119,
898 [http://dx.doi.org/10.1016/S0304-4203\(00\)00022-0](http://dx.doi.org/10.1016/S0304-4203(00)00022-0), 2000.

899 Marchitto, T. M., Curry, W. B., and Oppo, D. W.: Zinc concentrations in benthic
900 foraminifera reflect seawater chemistry, *Paleoceanography*, 15, 299-306,
901 10.1029/1999PA000420, 2000.

902 Marchitto, T. M., Lynch-Stieglitz, J., and Hemming, S. R.: Deep Pacific CaCO₃
903 compensation and glacial–interglacial atmospheric CO₂, *Earth and Planetary Science Letters*,
904 231, 317-336, <http://dx.doi.org/10.1016/j.epsl.2004.12.024>, 2005.

905 McCorkle, D. C., Martin, P. A., Lea, D. W., and Klinkhammer, G. P.: Evidence of a
906 dissolution effect on benthic foraminiferal shell chemistry: $\delta^{13}\text{C}$, Cd/Ca, Ba/Ca, and Sr/Ca
907 results from the Ontong Java Plateau, *Paleoceanography*, 10, 699-714, 10.1029/95PA01427,
908 1995.

909 Mewes, A., Langer, G., Reichert, G.-J., De Nooijer, L. J., Nehrke, G., and Bijma, J.: The
910 impact of Mg contents on Sr partitioning in benthic foraminifers, *Chemical Geology*, 412, 92-
911 98, <http://dx.doi.org/10.1016/j.chemgeo.2015.06.026>, 2015.

912 Mezger, E. M., de Nooijer, L. J., Boer, W., Brummer, G. J. A., and Reichart, G. J.: Salinity
913 controls on Na incorporation in Red Sea planktonic foraminifera, *Paleoceanography*,
914 10.1002/2016PA003052, 2016.

915 Mucci, A., and Morse, J. W.: The incorporation of Mg^{2+} and Sr^{2+} into calcite overgrowths:
916 influences of growth rate and solution composition, *Geochimica et Cosmochimica Acta*, 47,
917 217-233, [http://dx.doi.org/10.1016/0016-7037\(83\)90135-7](http://dx.doi.org/10.1016/0016-7037(83)90135-7), 1983.

918 Nardelli, M. P., Malferrari, D., Ferretti, A., Bartolini, A., Sabbatini, A., and Negri, A.: Zinc
919 incorporation in the miliolid foraminifer *Pseudotriloculina rotunda* under laboratory conditions,
920 *Marine Micropaleontology*, 126, 42-49, <http://dx.doi.org/10.1016/j.marmicro.2016.06.001>,
921 2016.

922 Nehrke, G., Keul, N., Langer, G., De Nooijer, L. J., Bijma, J., and Meibom, A.: A new model
923 for biomineralization and trace - element signatures of Foraminifera tests, *Biogeosciences*, 10,
924 6759-6767, 10.5194/bg-10-6759-2013, 2013.

925 Nürnberg, D., Bijma, J., and Hemleben, C.: Assessing the reliability of magnesium in
926 foraminiferal calcite as a proxy for water mass temperatures, *Geochimica et Cosmochimica*
927 *Acta*, 60, 803-814, 10.1016/0016-7037(95)00446-7, 1996.

928 Okai, T., Suzuki, A., Kawahata, H., Terashima, S., and Imai, N.: Preparation of a New
929 Geological Survey of Japan Geochemical Reference Material: Coral JCp-1, *Geostandards*
930 *newsletter*, 26, 95-99, 2002.

931 Okumura, M., and Kitano, Y.: Coprecipitation of alkali metal ions with calcium carbonate,
932 *Geochimica et Cosmochimica Acta*, 50, 49-58, [http://dx.doi.org/10.1016/0016-7037\(86\)90047-](http://dx.doi.org/10.1016/0016-7037(86)90047-5)
933 [5](http://dx.doi.org/10.1016/0016-7037(86)90047-5), 1986.

934 Parkhurst, D. L., and Appelo, C.: User's guide to PHREEQC (Version 2): A computer
935 program for speciation, batch-reaction, one-dimensional transport, and inverse geochemical
936 calculations, US Geol. Surv, Denver, Colorado, 1999.

937 Pawlowski, J., Holzmann, M., Berney, C., Fahrni, J., Gooday, A. J., Cedhagen, T., Habura,
938 A., and Bowser, S. S.: The evolution of early Foraminifera, Proc Natl Acad Sci U S A, 100,
939 11494-11498, 10.1073/pnas.2035132100, 2003.

940 Pierrot, D., Lewis, E., and Wallace, D. W. R.: MS Excel Program Developed for CO₂ System
941 Calculations, Carbon Dioxide Information Analysis Center, Oak Ridge National Laboratory,
942 U.S., 2006.

943 Reichart, G.-J., Jorissen, F., Anschutz, P., and Mason, P. R.: Single foraminiferal test
944 chemistry records the marine environment, Geology, 31, 355-358, 2003.

945 Russell, A. D., Hönisch, B., Spero, H. J., and Lea, D. W.: Effects of seawater carbonate ion
946 concentration and temperature on shell U, Mg, and Sr in cultured planktonic foraminifera,
947 Geochimica et Cosmochimica Acta, 68, 4347-4361, 10.1016/j.gca.2004.03.013, 2004.

948 Sanyal, A., Hemming, N. G., Broecker, W. S., Lea, D. W., Spero, H. J., and Hanson, G. N.:
949 Oceanic pH control on the boron isotopic composition of foraminifera: Evidence from culture
950 experiments, Paleoceanography, 11, 513-517, 1996.

951 Sather, W. A.: Selective Permeability of Voltage-Gated Calcium Channels, in: Voltage-
952 Gated Calcium Channels, Springer US, Boston, MA, 205-218, 2005.

953 Segev, E., and Erez, J.: Effect of Mg/Ca ratio in seawater on shell composition in shallow
954 benthic foraminifera, Geochemistry, Geophysics, Geosystems, 7, 10.1029/2005GC000969,
955 2006.

956 Ter Kuile, B., and Erez, J.: Uptake of inorganic carbon and internal carbon cycling in
957 symbiont-bearing benthonic foraminifera, Marine Biology, 94, 499-509, 1987.

958 Toyofuku, T., Suzuki, M., Suga, H., Sakai, S., Suzuki, A., Ishikawa, T., De Nooijer, L. J.,
959 Schiebel, R., Kawahata, H., and Kitazato, H.: Mg/Ca and $\delta^{18}\text{O}$ in the brackish shallow-water
960 benthic foraminifer *Ammonia 'beccarii'*, Marine Micropaleontology, 78, 113-120,
961 <http://dx.doi.org/10.1016/j.marmicro.2010.11.003>, 2011.

962 Toyofuku, T., Matsuo, M. Y., de Nooijer, L. J., Nagai, Y., Kawada, S., Fujita, K., Reichart,
963 G.-J., Nomaki, H., Tsuchiya, M., Sakaguchi, H., and Kitazato, H.: Proton pumping accompanies
964 calcification in foraminifera, Nature Communications, accepted.

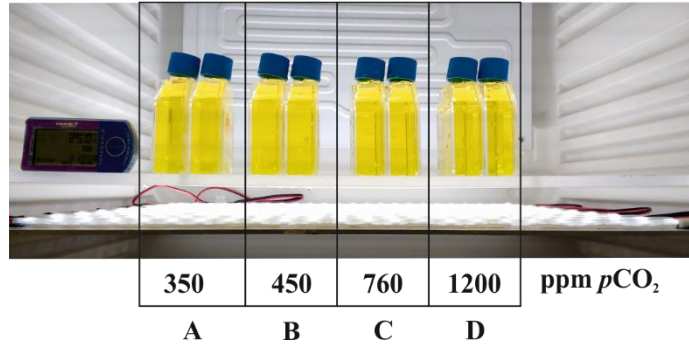
965 van Dijk, I., de Nooijer, L. J., Wolthers, M., and Reichart, G.-J.: Impacts of pH and $[\text{CO}_3^{2-}]$
966 on the incorporation of Zn in foraminiferal calcite, Geochimica et Cosmochimica Acta, 197,
967 263-277, <http://dx.doi.org/10.1016/j.gca.2016.10.031>, 2017.

968 Wit, J. C., De Nooijer, L. J., Barras, C., Jorissen, F. J., and Reichart, G. J.: A reappraisal of
969 the vital effect in cultured benthic foraminifer *Bulimina marginata* on Mg/Ca values: assessing
970 temperature uncertainty relationships, Biogeosciences, 9, 3693-3704, 10.5194/bg-9-3693-
971 2012, 2012.

972 Wit, J. C., De Nooijer, L. J., Wolthers, M., and Reichart, G. J.: A novel salinity proxy based
973 on Na incorporation into foraminiferal calcite, Biogeosciences, 10, 6375-6387, 10.5194/bg-10-
974 6375-2013, 2013.

975 Yu, J., and Elderfield, H.: Benthic foraminiferal B/Ca ratios reflect deep water carbonate
976 saturation state, Earth and Planetary Science Letters, 258, 73-86, 10.1016/j.epsl.2007.03.025,
977 2007.

978 Zeebe, R. E., and Sanyal, A.: Comparison of two potential strategies of planktonic
979 foraminifera for house building: Mg^{2+} or H^+ removal?, Geochimica et Cosmochimica Acta, 66,
980 1159-1169, [http://dx.doi.org/10.1016/S0016-7037\(01\)00852-3](http://dx.doi.org/10.1016/S0016-7037(01)00852-3), 2002.



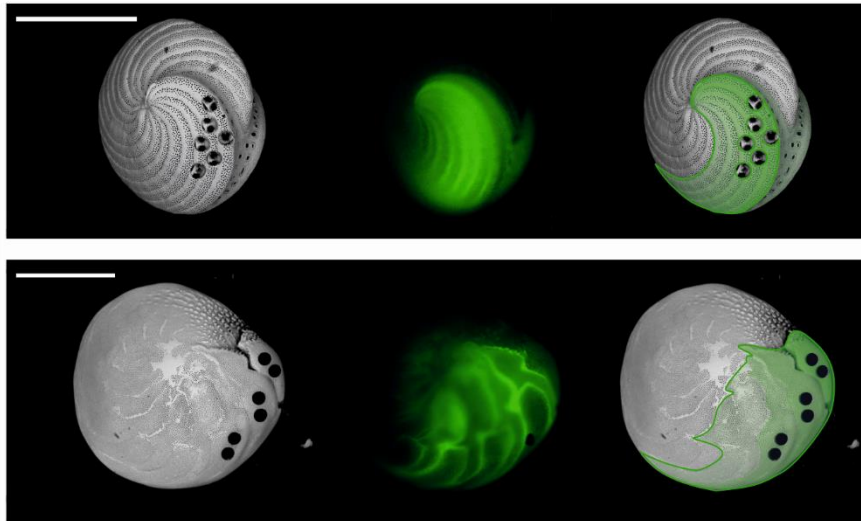
981

982

983

984

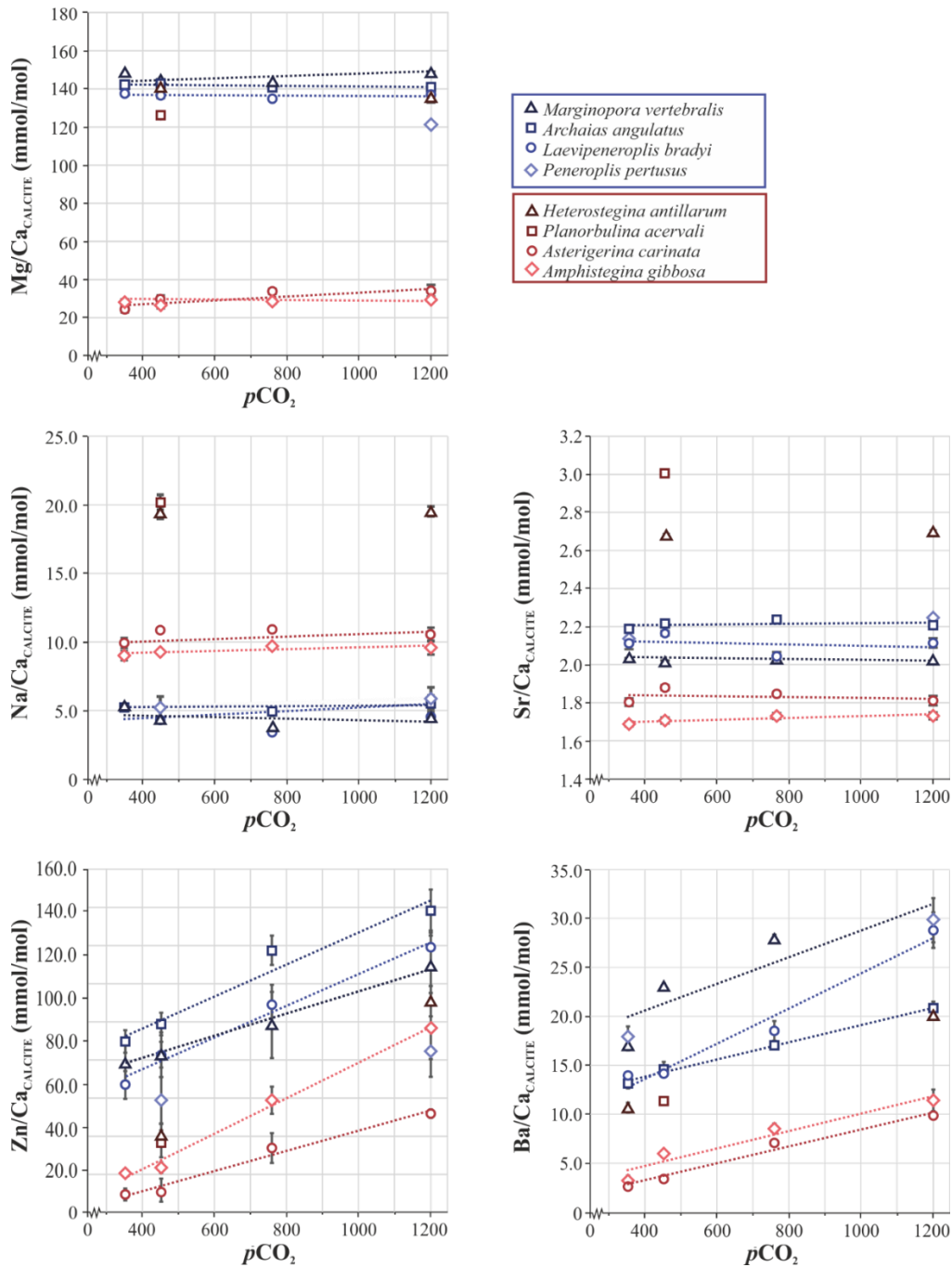
Figure 1. Photograph of the culture set-up. Four duplicate bottles with culture media (with calcein added) and adult specimens of foraminifera. Treatment with corresponding set-points are A=350 ppm, B=450 ppm, C=760 ppm, D=1200 ppm CO₂.



985

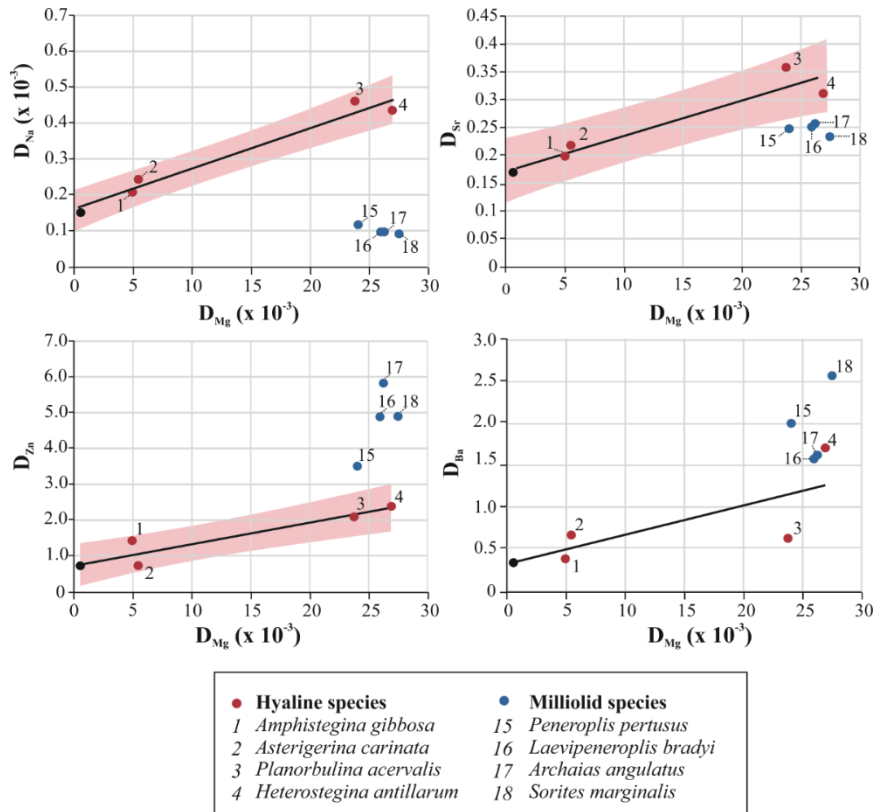
986 **Figure 2. SEM (left) and fluorescence microscope (middle) photographs of *A. angulatus* (top**
987 **series) and *A. gibbosa* (bottom series) to assess newly formed chambers for laser ablation (right).**

988 **Scale bar = 500 μm .**



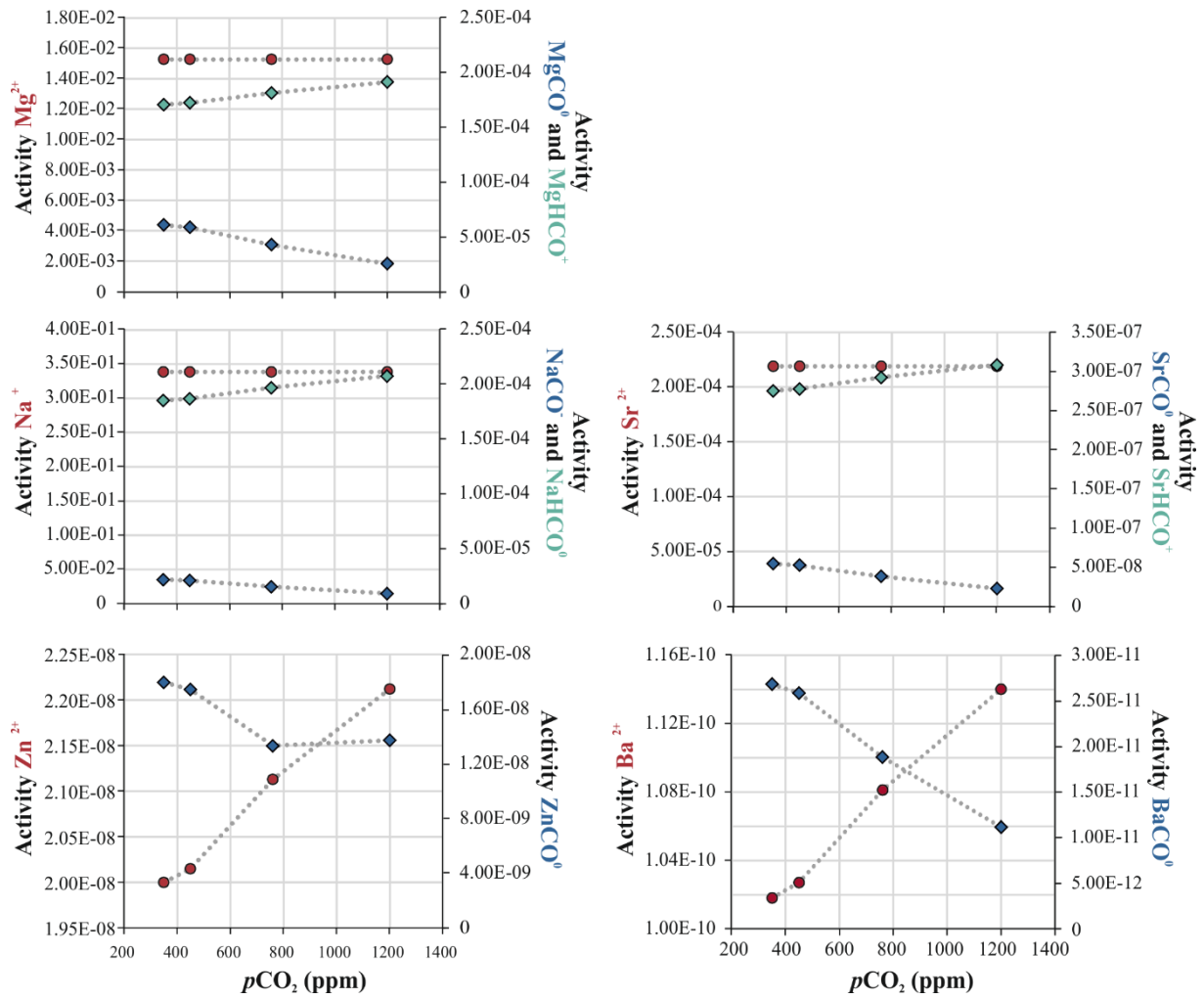
989

990 **Figure 3. Element to Ca ratios (\pm SE) of different species of foraminifera over a range of $p\text{CO}_2$**
 991 **values. In some cases, the error bar is smaller than the symbol. Porcelaneous species in blue**
 992 **(triangles = *S. marginalis*; squares = *A. angulatus*; circles = *L. bradyi*; squares = *P. pertusus*) and**
 993 **hyaline species in red (triangles = *H. antillarum*; squares = *P. acervalis*; circles = *A. carinata*;**
 994 **diamonds = *A. gibbosa*).**



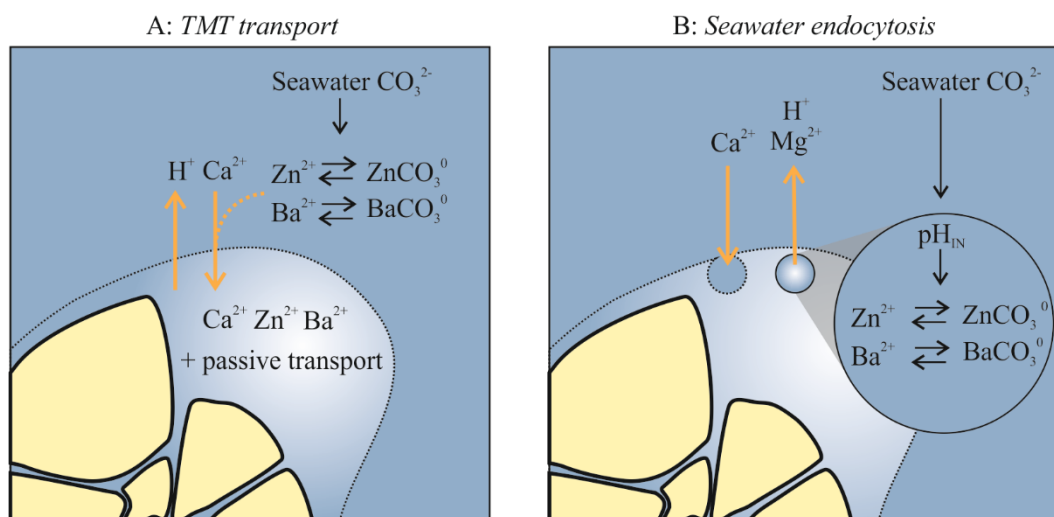
995

996 **Figure 4. Partition coefficient of Na, Sr, Zn and Ba versus D_{Mg} of hyaline (red symbols) and**
 997 **porcelaneous (blue symbols) species. Black lines represent linear trendlines. The 95% confidence**
 998 **intervals of signification trends ($p < 0.025$) are indicated in red. Black dots represent the NFHS, in-**
 999 **house carbonate standard, consisting of planktonic foraminifera. Numbers correspond to**
 1000 **foraminiferal species analyzed, numbers 5-14 and 18-21 represent values from previously**
 1001 **published species and are included in Figure S1 (supplementary information).**



1002

1003 **Figure 5. Speciation of Mg, Na, Sr, Zn and Ba in the different seawater treatments modelled in**
 1004 **PHREEQC (Parkhurst and Appelo, 1999). Activities of free ions (red) and element (E)-carbonate**
 1005 **complexes ($\text{ECO}_3 = \text{blue diamonds}$ and $\text{EHCO}_3 = \text{green diamonds}$).**



1006

1007 **Figure 6. Schematic overview of different mechanisms for ion transport during foraminiferal**
 1008 **calcification. Orange arrows indicate transport of ions. A) The transmembrane transport (TMT)**
 1009 **mixing model as proposed by Nehrke et al. (2013). The amount of free ions, e.g. Zn^{2+} and Ba^{2+} ,**
 1010 **available for transport by Ca^{2+} in exchange for protons (Toyofuku et al., accepted) is influenced**
 1011 **by speciation due to changes in seawater $[\text{CO}_3^{2-}]$. The composition of the seawater at the site of**
 1012 **calcification is determined by both TMT and passive transport B) Simplified overview of seawater**
 1013 **endocytosis (Bentov et al., 2009; Erez, 2003), where speciation of Zn^{2+} and Ba^{2+} is determined by**
 1014 **changes in internal pH (pH_{IN}), which changes with ambient seawater carbonate chemistry. Based**
 1015 **on our observations, panel A likely applies to hyaline species, whereas panel B represents**
 1016 **porcelaneous calcification.**

Treatment	Set-point	Measured		Calculated CO2SYS		
	$p\text{CO}_2$ ppm	TA $\mu\text{mol/kg}$	DIC $\mu\text{mol/kg}$	$[\text{CO}_3^{2-}]$ $\mu\text{mol/kg}$	pH (total scale)	Ω_{CALCITE}
A	350	2302.8±8.2	2007.5±10.7	220.7	8.06	5.4
B	450	2305.2±5.8	2021.3±12.5	200.0	8.01	4.9
C	760	2304.4±0.9	2100.8±13.4	153.7	7.87	3.7
D	1200	2300.3±0.7	2201.4±4.1	92.2	7.61	2.2

1017 **Table 1. Carbon parameters (TA= Total alkalinity, n=2, DIC=Dissolved Inorganic Carbon, n=2)**
1018 **with (relative) standard deviation of the culture water per treatment of the $p\text{CO}_2$ experiment.**
1019 **CO2SYS was used to calculate seawater carbonate ion concentration, calcite saturation state and**
1020 **pH from measured TA and DIC.**

Species	n measurements (n specimens)			
	A: 350 ppm	B: 450ppm	C:760 ppm	D:1200 ppm
<i>A. angulatus</i>	62 (19)	72 (21)	76 (21)	51 (14)
<i>S. marginalis</i>	48 (14)	49 (15)	57 (18)	33 (11)
<i>A. gibbosa</i>	106 (28)	126 (32)	75 (18)	59 (15)
<i>L. bradyi</i>	21 (5)	38 (13)	27 (5)	16 (4)
<i>A. carinata</i>	12 (2)	14 (1)	19 (4)	5 (1)
<i>P. pertusus</i>		12 (2)		11 (2)
<i>H. antillarum</i>		12 (1)		14 (2)
<i>P. acervalis</i>		8 (2)		
Total	187 (49)	331 (87)	254 (66)	189 (49)

1021 **Table 2. Total number of LA-ICP-MS measurements per species, per treatment (A-D).**

Species	$p\text{CO}_2$	Mg/Ca		Na/Ca		Sr/Ca		Zn/Ca		Ba/Ca	
		mmol/mol		mmol/mol		mmol/mol		$\mu\text{mol/mol}$		$\mu\text{mol/mol}$	
		Avg \pm SE	D_{Mg}	Avg \pm SE	D_{Na}	Avg \pm SE	D_{Sr}	Avg \pm SE	D_{Zn}	Avg \pm SE	D_{Ba}
		$\times 10^{-3}$		$\times 10^{-3}$							
Porcelaneous species											
<i>A. angulatus</i>	350	139.4 \pm 0.6 ^a	26.6	5.2 \pm 0.1 ^a	0.12	2.2 \pm 0.02 ^a	0.25	80.0 \pm 5.1 ^a	5.3	13.2 \pm 0.5 ^a	1.5
	450	137.7 \pm 0.5 ^b	26.3	4.3 \pm 0.1 ^b	0.10	2.2 \pm 0.01 ^a	0.26	88.1 \pm 5.2 ^b	5.8	14.6 \pm 0.5 ^b	1.6
	760	137.4 \pm 0.7 ^b	26.2	4.9 \pm 0.1 ^c	0.11	2.2 \pm 0.01 ^a	0.26	122.6 \pm 7.0 ^c	8.1	17.0 \pm 0.6 ^b	1.9
	1200	138.6 \pm 1.1 ^a	26.4	5.4 \pm 0.2 ^a	0.12	2.2 \pm 0.02 ^a	0.26	140.8 \pm 9.9 ^d	9.3	20.9 \pm 0.2 ^c	2.3
<i>S. marginalis</i>	350	147.7 \pm 0.6 ^a	28.2	4.8 \pm 0.1 ^a	0.11	2.0 \pm 0.01 ^a	0.24	70.0 \pm 10.1 ^a	4.6	17.0 \pm 0.5 ^a	1.9
	450	144.2 \pm 0.8 ^b	27.5	4.1 \pm 0.1 ^b	0.09	2.0 \pm 0.01 ^a	0.23	74.0 \pm 10.6 ^b	4.9	23.1 \pm 0.5 ^b	2.6
	760	143.0 \pm 0.6 ^a	27.3	3.8 \pm 0.1 ^a	0.09	2.0 \pm 0.01 ^a	0.23	87.7 \pm 15.5 ^c	5.8	27.9 \pm 0.6 ^c	3.1
	1200	148.3 \pm 0.5 ^b	28.3	4.5 \pm 0.2 ^c	0.10	2.0 \pm 0.01 ^a	0.23	115.6 \pm 15.3 ^d	7.6	30.1 \pm 0.2 ^d	3.3
<i>L. bradyi</i>	350	137.8 \pm 1.3 ^a	26.3	5.2 \pm 0.2 ^c	0.12	2.1 \pm 0.03 ^a	0.24	60.0 \pm 6.5 ^a	4.0	14.0 \pm 0.5 ^a	1.5
	450	136.2 \pm 0.7 ^a	26.0	4.3 \pm 0.1 ^b	0.10	2.2 \pm 0.01 ^b	0.25	73.8 \pm 6.0 ^b	4.9	14.2 \pm 0.5 ^a	1.6
	760	134.4 \pm 1.2 ^b	25.6	3.4 \pm 0.1 ^a	0.08	2.0 \pm 0.02 ^c	0.24	97.5 \pm 9.4 ^c	6.4	18.5 \pm 0.6 ^b	2.1
	1200	136.9 \pm 1.1 ^a	26.1	6.2 \pm 0.2 ^d	0.14	2.1 \pm 0.02 ^a	0.24	124.2 \pm 7.8 ^d	8.2	28.8 \pm 0.2 ^c	3.2
<i>P. pertusus</i>	350										
	450	126.1 \pm 1.8 ^a	24.0	5.2 \pm 0.3 ^a	0.12	2.1 \pm 0.07 ^a	0.25	53.0 \pm 10.8 ^a	3.5	18.0 \pm 0.5 ^a	2.0
	760										
	1200	121.3 \pm 1.0 ^a	23.1	5.8 \pm 0.2 ^a	0.13	2.2 \pm 0.02 ^a	0.26	75.5 \pm 11.9 ^b	5.0	29.8 \pm 0.2 ^b	3.3

Hyaline species											
<i>H. antillarum</i>	350										
	450	141.3±0.3 ^a	26.9	19.4±0.5 ^a	0.44	2.7±0.02 ^a	0.31	36.0±14.7 ^a	2.4	10.7±0.5 ^a	1.2
	760										
	1200	136.9±1.6 ^a	26.1	19.5±0.4 ^a	0.44	2.7±0.02 ^a	0.31	97.0±18.3 ^b	6.4	20.1±0.2 ^b	2.2
<i>P. acervalis</i>	350										
	450	139.1±1.2	26.5	19.5±0.7	0.46	3.1±0.02	0.36	31.6±6.6	2.1	11.3±0.5	1.3
	760										
	1200										
<i>A. carinata</i>	350	23.6±1.5 ^a	4.5	9.9±0.4 ^a	0.22	1.8±0.02 ^a	0.21	9.0±2.6 ^a	0.6	3.2±0.5 ^a	0.4
	450	28.5±2.4 ^b	5.4	10.8±0.1 ^a	0.24	1.9±0.01 ^a	0.22	10.9±5.5 ^a	0.7	6.0±0.5 ^b	0.7
	760	33.1±1.2 ^b	6.3	10.9±0.2 ^a	0.24	1.8±0.01 ^a	0.21	30.7±7.0 ^b	2.0	8.5±0.6 ^c	0.9
	1200	33.5±3.1 ^b	6.4	10.6±0.5 ^a	0.24	1.8±0.03 ^a	0.21	46.4±2.1 ^b	3.1	11.4±0.2 ^d	1.3
<i>A. gibbosa</i>	350	27.8±0.5 ^a	5.3	9.0±0.1 ^a	0.20	1.7±0.01 ^a	0.20	19.0±1.8 ^a	1.3	2.7±0.5 ^a	0.3
	450	25.9±0.6 ^b	4.9	9.2±0.1 ^a	0.21	1.7±0.02 ^a	0.20	21.5±2.5 ^b	1.4	3.4±0.5 ^a	0.4
	760	28.2±0.7 ^a	5.4	9.7±0.1 ^b	0.22	1.7±0.02 ^a	0.20	52.8±6.1 ^c	3.5	7.1±0.6 ^b	0.8
	1200	28.7±0.6 ^a	5.5	9.6±0.1 ^b	0.21	1.7±0.02 ^a	0.20	85.8±11.3 ^d	5.7	9.9±0.2 ^c	1.1

1022 **Table 3. Overview of element to Ca ratios in foraminiferal calcite (Avg=average; SE=standard**
1023 **error) and partition coefficients D_E , with D_E of ambient conditions (treatment B) in bold. Letters**
1024 **(^a to ^d) indicate (per species per E/Ca) groups that are statistical different (one-way ANOVA).**

Species	Zn/Ca		Ba/Ca	
	R ²	p-value	R ²	p-value
<i>S. marginalis</i>	0.99	<0.0005	0.81	<0.025
<i>A. angulatus</i>	0.95	<0.0025	0.99	<0.0005
<i>L. bradyi</i>	0.98	<0.0005	0.97	<0.0025
<i>A. carinata</i>	0.98	<0.001	0.94	<0.005
<i>A. gibbosa</i>	0.99	<0.0005	0.98	<0.001

1025 **Table 4. Regression and p-values of foraminiferal Zn/Ca and Ba/Ca versus $p\text{CO}_2$ values of**
1026 **different species (Fig. 4).**